Superior Colliculus to VTA pathway controls orienting behavior during conspecific interaction.

One sentence summary: Distinct ventral tegmental area dopaminergic pathways encode for complementary aspects of social behavior in mice.

Clément Prévost-Solié[1]*, Alessandro Contestabile[1]*, Stefano Musardo[1], Chieko Huber[1], Sebastiano Bariselli[1], Alan Carleton[1] and Camilla Bellone[1]

[1]Department of Basic Neuroscience, University of Geneva; 1, Rue Michel-Servet, 1205 Geneve, Switzerland.

*Equal contribution

Correspondence to: Camilla.bellone@unige.ch

Abstract

Social behaviors are highly important in mammals as conspecific interaction impairments are symptomatic of neuropsychiatric diseases. Several neural circuit mechanisms underlying the regulation of social behaviors have been described. Among them, dopamine (DA) neurons in the Ventral Tegmental Area (VTA) have been implicated in modulating the rewarding properties of conspecific interaction. However, how DA neurons receive information related to conspecifics is still an open question. In this study, we identified that Superior Colliculus (SC) neurons projecting to the VTA decrease their activity during conspecific interaction. Using optogenetic approaches, we demonstrated that SC – VTA pathway controls orientation towards unfamiliar conspecifics and regulates social interaction while Anterior Cortex (AC) to VTA pathway promotes conspecific interaction without affecting orienting behaviors towards the conspecific. Moreover, we show that contrary to AC pathway, SC projects onto VTA DA neurons that send inputs to dorsolateral striatum (DLS). Photostimulation of VTA to DLS pathway decreases interaction, mimicking SC to VTA stimulation. Our work not only delineates a previously unknown role of SC–VTA–DLS pathway in controlling orienting behavior during conspecific interaction, but also supports the hypothesis that different VTA DA neurons subpopulations play a specific role in social behavior.

Introduction

The term "social interaction" describes interactions with conspecifics, which are highly complex behaviors guided by environmental and internal stimuli. When entering in a novel setting, individuals need to constantly integrate external sensory cues with internal states to properly orient towards conspecifics. These processes prepare the subject to deal with the different situations that a stimulus may evoke[1]. At a biological level, several brain regions are functionally relevant for conspecific interaction. Therefore, to fully understand the complexity of this behavior, the neurocircuitry underlying specific aspects of social interaction needs to be precisely investigated.

Because of its role in reward and motivation, the ventral tegmental area (VTA) and dopamine (DA) have long been implicated in affiliative interactions[2,3]. Indeed, DA release peaks upon initial contact with a conspecific and habituates upon subsequent presentation of the same stimulus[3]. More recently, fiber photometry approaches have shown that activity dynamics of VTA to nucleus accumbens (NAc) encode key aspects of social interaction[4]. Interestingly, while stimulation of VTA DA neurons projecting to the NAc (VTA^{DA} – NAc) increases interaction[4], chemogenetic inhibition of VTA DA neurons attenuates both the exploration and the reinforcing properties of unfamiliar conspecifics in mice[5]. However, the circuit mechanisms that modulate the activity of DA neurons during social interaction are still largely unknown.

Social cues are environmental salient stimuli that capture attention and favor orientation. After orienting towards a conspecific, the individual evaluates the situation and decides whether to initiate or to avoid the interaction. In this context, orienting represents the first and necessary step to engage in social behavior. Remarkably, unexpected biologically-relevant salient events evoke DA neuron responses in several species[6, 7]. Indeed, midbrain DA neurons respond with short-latency to different sensory cues[8] and their response habituate rapidly when the stimulus is repeated. Several studies have provided evidence that a subcortical structure in the midbrain, the Superior Colliculus (SC), is a source of short-latency visual inputs to midbrain DA neurons [9,10,11,12]. SC is an evolutionary conserved midbrain structure that is activated by biological salient stimuli independently of their valence[13] and plays a key role in controlling orientation and spatial attention[14,15,16]. Recently, it has been shown that SC sends excitatory projections onto VTA GABA[17] neurons to control

defensive behavior while SC inputs onto VTA DA neurons might contribute to reinforcement learning. However, whether SC conveys information to VTA DA neurons during social orienting, thus having a pivotal role in conspecific interaction, remains unknown.

Midbrain DA neurons cluster in different subpopulations that regulate emotional, cognitive and motor functions. Efferent projections mainly target the striatum and the cortex and several afferent projections have been anatomically identified. Interestingly, it is generally assumed that DA neurons in the VTA project to the ventral part of the striatum, while DA neurons in the substantia nigra (SN) send projection to the dorsal striatum. However, a gradient distribution of DA cells projecting to the ventromedial, central and dorsolateral striatum has been observed[18]. Through a spiral input – output connection between the striatum and the midbrain, information flows from limbic to motor circuits providing a mechanism by which motivation can influence decision-making and action performance[19]. Thus, this cross-talk between circuits would be important to adjust behavior in function of novel information. However, whether different loops within the midbrain circuit play a different role in conspecific interaction is still largely unknown.

Here we show that the neuronal activity of identified SC to VTA input neurons (SC – VTA) decreases upon exposure to unfamiliar conspecifics. Furthermore, optogenetic stimulation of SC – VTA pathway disturbs orientation towards social stimuli and decreases conspecific interaction, while optogenetic inhibition of this pathway promotes investigation and increases orienting behavior towards the unfamiliar conspecific. Interestingly, stimulation of the previously described Anterior Cortex (AC) to VTA input pathway (AC – VTA;[20]) increases conspecific interaction without affecting orientation, suggesting complementary involvement of SC – VTA and AC – VTA pathways in social behaviors. Remarkably, we found that VTA DA neurons receiving SC projections mainly provide inputs to dorsolateral striatum (DLS). Optogenetic stimulation of this VTA^{DA} – DLS pathway, contrary to VTA^{DA} – NAc circuit that receives inputs from AC, decreases conspecific interaction similarly to SC – VTA projections stimulation.

Results

VTA receives projection from SC

To anatomically assess the presence of a projection from SC to VTA, we first injected an adeno-associated virus (AAV) expressing a yellow fluorescent protein (eYFP; AAV5-hSyn-eYFP) in the SC (**Fig. 1a-b**), and we observed SC axons in the VTA (**Fig. 1b'**). To identify the anatomical position of SC neurons projecting to VTA, we injected a retrograde virus (CAV-) expressing Cre in the VTA and a Cre-dependent AAV virus expressing mCherry (AAV5-hSyn-DIO-mCherry) in the SC (**Fig. 1c**). This experiment revealed that SC neurons projecting to the VTA are predominately located in the intermediate and deep layers (**Fig. 1d, f**). Furthermore, immunohistochemistry analysis indicated that 88,1% of SC neurons projecting to the VTA are CaMKIIα positive (**Fig. 1e, f**), suggesting a prevalent excitatory connection between SC and VTA. To explore the functional connectivity of SC – VTA projections, we performed whole-cell patch clamp recordings in VTA acute slices obtained from mice injected with AAV5-hSyn-ChR2-eYFP in SC (**Fig. 1g, h**). As expected, optogenetic stimulation of axons in the VTA evoked excitatory postsynaptic currents (oEPSCs) in 48.28% of DA neurons while inhibitory postsynaptic currents (oIPSCs) were recorded only in 17.24% of DA neurons (**Fig. 1i**). These data indicate that the SC projections to VTA DA neurons are mainly excitatory.

In vivo calcium activity of SC to VTA pathway during conspecific interaction

To illustrate how calcium dynamics of SC neurons projecting to the VTA change during real-time exploration of unfamiliar stimuli associated with social and non-social behavior, we injected a retrograde AAV-expressing Cre in the VTA and a Cre dependent AAV carrying GCaMP6f in the SC (**Fig. 2a, b**). We then monitored the activity of SC neurons projecting to the VTA and expressing the genetically encoded calcium indicator GCaMP6f using microendoscopic calcium imaging during conspecific interaction (**Fig. 2b-d**). First, we placed a freely moving mouse in an unfamiliar environment (home cage-like arena) for 5 minutes and we acquired baseline GCaMP6f fluorescence from SC neurons projecting to the VTA. Afterwards, we introduced in the same arena an unfamiliar sex-matched conspecific and recorded the calcium transients during a 5-minute-long social interaction session. The experiment was repeated 24h after, re-acquiring a baseline (baseline 2) and using an unfamiliar inanimate object as stimulus instead of the conspecific (**Fig. 2e**). A population of neurons displays higher firing rate in baseline condition compared to conspecific and non-

conspecific interactions (**Fig. 2f**). However, we noticed a decrease in the percentage of active neurons during social interaction only (**Fig. 2g**). These experiments suggest that SC – VTA pathway is active during the exploration of an unfamiliar environment and becomes more silent when an unfamiliar stimulus is introduced in the cage.

SC to VTA pathway bidirectionally controls conspecific interaction

To investigate the role of SC – VTA pathway during conspecific interaction, we used optogenetic activation and inhibition interventions. We injected red light-sensitive optogenetic inhibitor Jaws (AAV-hSyn-Jaws-GFP or AAV-hSyn-eYFP as control) or the blue-light sensitive ChR2 (AAV-hSyn-ChR2-eYFP or AAV-hSyn-eYFP as control) in the SC followed by optic fiber implantation over the VTA to inhibit or stimulate SC axon terminals (**Fig. 3a-c'**). We first placed the mice in a home cage like arena and, after 3 min baseline, we exposed the experimental mouse to an unfamiliar conspecific for 2 min concomitantly or not with photoinhibition or photostimulation. The experiment was then repeated with another unfamiliar conspecific after 3 h delay (counterbalanced), and we compared the total time spent in investigation (time sniffing) between light OFF and light ON epochs (**Fig. 3d**). Interestingly, while photoinhibition of SC – VTA pathway significantly increased investigation time in Jaws-expressing mice without affecting the eYFP-control group (**Fig. 3e, f**), photostimulation of this pathway in ChR2-expressing mice decreased time interaction (**Fig. 3g, h**). In order to better dissect the behavioural effects of SC – VTA pathway manipulation, we analyzed detailed aspects of social and non-social behavior sequences during both light OFF and light ON epochs. Although we did not find differences in self-grooming or rearing behavior, photostimulation or photoinhibition elicited opposite changes mainly in "following" behavior between light ON and OFF conditions **(Fig. 3i-p)**.

We next tested whether photoinhibition and photostimulation of SC – VTA pathway interfere with object exploration. Following the same experimental design, we exposed the eYFP-control, Jaws-expressing and ChR2-expressing mice to an unfamiliar inanimate object (**Supplementary Fig. 1a**). The analysis of the time spent in exploring the object did not reveal differences between photoinhibition or photostimulation conditions and eYFP-control groups (**Supplementary Fig. 1b-c**). These data strongly suggest that SC – VTA pathway plays an important role in conspecific interaction.

SC to VTA pathway controls orientation

Using the free social interaction paradigm described previously, we noticed that the eYFP-expressing mice quickly habituate to the stimulus and spend less time investigating the conspecific through the 2 minutes of interaction (**Fig. 4a-b**). We analyzed whether changes in conspecific interaction observed upon SC – VTA manipulations were the consequence of an aberrant initiation of social contact. Thus, we plotted the time course of the time spent investigating the unfamiliar conspecific. Interestingly, Jaws-expressing mice prolonged while ChR2-expressing mice decreased their interaction time over the first 100 seconds when comparing light ON and OFF conditions (**Fig. 4a-b**). These results suggest that social contact initiation is controlled by SC – VTA pathway.

When an unfamiliar conspecific is introduced in the environment, the experimental mouse typically stops the ongoing action to re-orient its attention towards the stimulus, right before or while initiating a bout of interaction. To capture this attentional shift during social exposure, we calculated the head orientation (ω) as the angle formed between experimental mouse body center – head vector and unfamiliar conspecific body center (**Fig. 4c**). In eYFP-control mice, the angle of head orientation follows the interaction time and rapidly increases during the first 100 seconds of the task, revealing reduced orientation towards the unfamiliar conspecific across the session (**Fig. 3d, e**). This result reflects an increased attention directed towards the unfamiliar conspecific during the first instants of social interaction. Interestingly, photoinhibition of SC – VTA pathway does not affect orientation towards the social stimulus during the first moments of interaction (**Fig. 4d**) while photostimulation decreases orientation (**Fig. 4e**). Thereby, photoinhibition and photostimulation of SC – VTA pathway altered head orientation compared to light OFF epochs in opposite ways. Furthermore, we observed a significant inversed linear correlation across the session between interaction time and head-orientation angle for eYFP-control and Jaws-expressing animals during both light OFF and light ON epochs (**Fig. 4f, g**). These results indicate that head orientation and social contact are tightly related features of social behavior. Interestingly, we observed a loss of correlation between head orientation and social contacts during light ON epochs in ChR2-expressing mice (**Fig. 4g**), reinforcing the idea that a reduction of SC – VTA pathway activity is necessary for appropriate orienting towards social stimuli. Finally, we quantified the proportion of time spent by the experimental stimulus with the head directed towards social

stimuli for a range of angles, from 10 to 180 degrees. We observed that Jaws-expressing mice spent more time between 30 and 110 degrees orientation angles, (**Fig. 4h**) while ChR2-expressing mice spent significantly less time during light ON compared to light OFF epochs (**Fig. 4i**). Interestingly, the head orientation analysis during object exploration (**Supplementary Fig. 1d**) reveled a difference between light ON and light OFF epochs only for ChR2-expressing mice (**Supplementary Fig. 1e-f**). In fact, these animals presented a decreased orientation of the head towards the unfamiliar object (**Supplementary Fig. 1f**) as observed in the social interaction task (**Fig. 4e**). These data further support the hypothesis that the activity of SC – VTA pathway controls orientation behaviors towards stimuli and is particularly relevant for conspecific interaction.

SC to VTA pathway modulates social novelty exploration

We have previously shown that DA neuron activity is necessary to promote exploration of an unfamiliar conspecific[5] and the experiments performed so far suggest that SC – VTA pathway controls orientation and is necessary to favor interaction with an unfamiliar conspecific. To investigate whether this pathway also controls sociability and social novelty exploration, we injected ChR2 in the SC, implanted fiber optics in the VTA and performed three-chambered interaction task[5] with those mice (**Supplementary Fig. 2a**). During social preference, while eYFP-control mice spent more time in close contact with an unfamiliar conspecific compared to an object during both light OFF and light ON period, SC – VTA stimulation in ChR2-expressing mice abolished social preference during light ON epochs (**Supplementary Fig. 2b**). Furthermore, during the social novelty phase, while eYFP-control mice spent more time in close contact with an unfamiliar conspecific compared to a familiar one during both light OFF and light ON epochs, stimulation of SC – VTA pathway in ChR2-expressing mice, not only abolished social novelty preference, but promoted the exploration of a familiar mouse (**Supplementary Fig. 2c**).

To better investigate whether stimulation of SC – VTA pathway interferes with unfamiliar conspecific exploration, we performed a long-term habituation/novelty exploration paradigm. Specifically, we assessed the time spent in interaction upon repeated exposure to the same mouse for 4 days (habituation) and the subsequent response to an unfamiliar conspecific at the 5th day during photostimulation **(Supplementary Fig. 2d**). At day 5, while eYFP-control mice increased the time spent in social exploration, ChR2-expressing mice did not engage in longer social exploration compared to day 4 (**Supplementary Fig. 2e**). Finally, we observed

significant differences when directly comparing eYFP-control and ChR2-expressing mice using time social interaction index (**Supplementary Fig. 2f**).

To confirm that SC – VTA pathway is implicated specifically in exploration towards an unfamiliar conspecific, we photostimulated and photoinhibited SC – VTA pathway during familiar conspecific interaction (**Supplementary Fig. 3a**). We observed that in eYFP-control, Jaws-expressing and ChR2-expressing mice the time interaction decreased between explorations of unfamiliar followed by familiar conspecific trials (T1 versus T2; **Supplementary Fig. 3b-e**).

Altogether these findings suggest that affecting orientation during initial contact with conspecific is sufficient to alter the interaction with an unfamiliar conspecific, leaving the interaction with familiar stimulus intact.

SC – VTA pathway stimulation is not reinforcing *per se*

To test whether manipulation of SC-VTA pathway changes exploratory behavior non-associated with a stimulus, eYFP-control, Jaws-expressing or ChR2-expressing mice were placed in an open field for 10 min to assess their locomotor activity (**Supplementary Fig. 4a**). No changes in distance moved where observed in Jaws-expressing mice between light OFF and light ON epochs (**Supplementary Fig. 4b-d**). On the other hand, although we did not observe significant differences between light OFF and light ON epochs using a within-group analysis, ChR2-expressing mice increased their distance moved relative to control animals upon SC terminal stimulation (**Supplementary Fig. 4e-g**). To exclude anxiolytic effects due to SC – VTA pathway stimulation, we measured the time spent in the center of the arena, which was similar between eYFP-control, Jaws-expressing and ChR2-expressing mice (**Supplementary Fig. 4h-j**). We finally tested whether manipulation of SC – VTA pathway would support real-time place preference. Animals were placed into a two-chambered arena, where only one chamber was paired with optical stimulation (**Supplementary Fig. 4k**). eYFP-control, Jaws-expressing or ChR2-expressing mice spent a comparable amount of time in each chamber (**Supplementary Fig. 4l-m**).

These data indicate that, while manipulation of SC – VTA pathway does not induce preference or avoidance for a neutral environment or changes in anxiety levels, it controls orientation during conspecific contacts and influence time interaction with an unfamiliar social stimulus.

Optogenetic manipulation of AC to VTA pathway during conspecific interaction

Our data so far indicate that the appropriate orientation towards an unfamiliar conspecific, supported by SC-VTA pathway function, is necessary for social interaction. Once mice enter in contact, the interaction might acquire a positive valence, which is necessary for a protracted social exploration. Thus, it is possible that while SC – VTA pathway contributes to change conspecific interaction through orientation, other inputs might underlie other aspects of social behaviour. AC regions, including insular, orbitofrontal cortexes and prefrontal cortex project to the VTA and altogether form a reinforcing pathway[20]. Because of the different functions encoded by AC and SC, we next asked whether SC – VTA and AC – VTA pathways contribute to social orienting and social maintenance, respectively. To test this hypothesis, we injected AAV-hSyn-ChR2-eYFP or AAV-hSyn-eYFP in the AC, followed by optic fibers implantation in the VTA (**Fig. 5a-c'**). Then, as in the task described previously, we subsequently exposed the eYFP-control and ChR2-expressing mice to two different unfamiliar conspecifics (**Fig. 5d**). We observed that ChR2-expressing mice increased time interaction during photostimulation of the AC – VTA pathway, while no changes occurred in the eYFP-control group (**Fig. 5e-f**). These data indicate that AC – VTA pathway promotes social interaction. To test the specificity of this pathway in sustaining social interaction, relative to the SC – VTA inputs rather involved in social orienting, we compared the proportion of time spent by the experimental animals with head directed towards the conspecific stimuli. Remarkably, we did not observe differences between photostimulation conditions in eYFP-control and ChR2-expressing mice (**Fig. 5g**). These results strongly suggest that, contrary to manipulation of SC – VTA pathway, AC – VTA circuit stimulation promotes the maintenance of conspecific interaction without affecting orientation.

AC – VTA^{DA} – NAc and SC – VTA^{DA} – DLS have different effects on unfamiliar conspecific interaction

These data not only indicate that SC – VTA pathway plays a specific role during interaction, but also show that SC – VTA and AC – VTA circuits control different aspects of social behavior. To further explore the complementary roles of SC and AC to VTA pathways, we tested the hypothesis that these regions are targeting anatomically distinct neuronal sub-populations in the VTA. Midbrain DA neuron axons innervate the striatum with a gradient distribution of cells projecting to the ventromedial central and dorsolateral striatum[19]. We

therefore injected Cholera Toxin Subunit B (CTB)-488 in the Nucleus Accumbens (NAc) and CTB-555 in the dorsolateral part of the striatum (DLS) and we imaged the VTA (**Fig. 6a-d**). As previously reported [21], we found that VTA neurons projecting to the NAc and to the DLS constitute two non-overlapping neuronal populations (**Fig. 6c-e**). Furthermore, we used optogenetics combined with retrograde tracing to investigate the functional connectivity of the SC – VTA^{DA} – DLS pathway. We injected retrograde AAVrg-FLEX-tdTomato in either DLS or NAc in DAT-Cre mice to label distinct VTA DA projecting neurons. Within the same animals, we injected AAV-hSyn-ChR2-eYFP in the SC to assess biases in input connectivity based on output-specificity. We performed whole cell patch clamp recordings from identified VTA DA projecting neurons (**Fig. 6f**) and found that SC makes functional synapses onto VTA DA neurons projecting to the DLS with 35.71 % of excitatory connections (**Fig. 6g**). However, VTA DA neurons projecting to the NAc are poorly connected with the SC cells (**Fig. 6g**). As a control, we explored another subpopulation of VTA DA neurons projecting to the tail of the striatum (TS), making very few connections with SC neurons as well (**Fig. 6g**).

Finally, since it has been shown that AC makes monosynaptic inputs onto NAc-projecting VTA DA neurons, we hypothesized that VTA^{DA} – DLS and VTA^{DA} – NAc pathways play different roles during conspecific interaction. Thereby, photostimulation of these pathways would mimic the effects presented previously by stimulating SC – VTA and AC – VTA pathways, respectively. To confirm this hypothesis, we injected Cre-dependent ChR2 (AAV5-EF1α-DIO-ChR2-eYFP) or Cre-dependent eYFP (AAV5-Ef1α-DIO-eYFP) in DAT-Cre mice followed by optic fiber implantation over either DLS or NAc (**Fig. 6h-i**). Experimental mice underwent the same behavioral protocol described previously (**Fig. 6j**). As expected, photostimulation of VTA^{DA} – NAc pathway in ChR2-expressing mice increased time interaction between conspecifics while no changes were observed in eYFP-control group (**Fig. 6k-l** and **n**)[4]. Remarkably, photostimulation of VTA^{DA} – DLS in ChR2-expressing mice decreases time sniffing the unfamiliar conspecific (**Fig. 6m-n**), recapitulating the effects of SC – VTA pathway stimulation. Altogether these data indicate that AC – VTA^{DA} – NAc and SC – VTA^{DA} – DS play distinct but complementary roles in social interaction.

Discussion

The present study examines the role of the SC – VTA pathway for unfamiliar conspecific interaction. We parsed the involvement of two different VTA pathways in distinct, but not mutually exclusive, components of social interaction: while SC – VTA pathway encodes orientation towards an unfamiliar conspecific, AC – VTA circuit regulates the maintenance of social interaction.

Interaction between conspecific consists of distinct, but subsequent and complementary, components. At first, an individual detects the presence of other conspecifics and then estimates the valence of a hypothetical interaction to make decisions on whether to initiate the contacts. After the first interaction, an individual updates the neuronal representation of the value associated with that interaction to guide its subsequent decisions [22] to or -not- to maintain that social contact. The mesolimbic system has been previously linked to social interaction and several studies strengthened the hypothesis that DA neurons of the VTA play an important role in different social behavior aspects[23]. However, whether distinct subclasses of DA neurons or different inputs onto VTA sub-serve these functions remained an open question. Our data support the hypothesis that different inputs converge to separate subclasses of VTA DA neurons and that each pathway independently encodes complementary aspects of conspecific interaction. Indeed, while the SC – VTA pathway provides the initial signal necessary to orient towards a conspecific, the AC – VTA pathway contributes to positive/incentive value assignment and therefore maintenance of social interaction.

SC is an evolutionary ancient structure organized in functionally and anatomically distinct layers. While the upper layers are exclusively visual, the medial and deeper layers have multisensory and motor functions[24]. It has been suggested that this structure, *via* different output projections, mediates both orienting and avoidance responses to novel sensory stimuli[13,15]. Moreover, SC lesions generally result in deficits in visual orientation, sensory neglect[25] and aberrant predatory responses[26]. Previous reports have shown that SC mediates visually-induced defensive behaviors. Indeed, the activity of excitatory neurons in the deep layers of the medial SC represents the saliency of the threat stimulus and is predictive of

escape behavior [27,28]. More specifically, the SC projections onto the VTA GABA neurons would promote "flight" behavior in threatening context[17].

Here, we demonstrated, for the first time, the importance of the SC in social contexts. In fact, our data show that SC – VTA pathway is activated during exploration of a novel environment and silenced when an unfamiliar social stimulus is introduced in the arena. Perturbing the physiological activity pattern of this pathway affects orientation and, consequently, social interaction. Thus, the activity of SC – VTA pathway is tightly tuned to environmental stimuli to heighten attention and favor orientation.

Midbrain DA neurons are located in two neighboring nuclei: the Substantia Nigra (SN) and the VTA [29] from where they project diffusely throughout the brain. Canonically, DA neurons are involved in reward-based learning, yet some studies observed that a subpopulation is activated by aversive stimuli[30,31,32]. These findings have led to the hypothesis that these DA neurons may signal "incentive salience" and facilitate a behavioural response when a salient stimulus is detected[33, 21]. Interestingly, it has been shown that short latency phasic responses can be elicited in DA neurons by unexpected rewards or by conditioned stimuli that predict the reward [34, 33, 35]. In this regard, different studies have shown that the midbrain SC directly projects to midbrain DA neurons and can relay reward-predictive sensory information to them [11,36]. In our study, we prove that SC projects to a subpopulation of VTA DA neurons that sends outputs to the DLS, thus pointing at the DA neurons as a relay node between the SC and the striatum. Interestingly, the looped circuit connecting the SC to the basal ganglia may be a "candidate mechanisms to perform the pre-attentive selections required to determine whether gaze should be shifted, and if so, to which stimulus"[16]. Our data therefore propose that, in the context of unfamiliar conspecific interaction, signals from the SC to the VTA DA neurons trigger orientation towards salient stimuli to favor interaction.

Social behavior involves a sequence of different actions: from interruption of the ongoing behavior, stimulus evaluation, decision-making and further exploration. In particular, social motivation is characterized by preferential orientation towards social stimuli, evaluation of the rewarding properties of conspecific interaction and effort to maintain social bonds [23]. Social motivation deficits play a central role in Autism Spectrum Disorders (ASDs), a neuropathology characterized by major social behavior alterations. Although evidence suggests that VTA is central to social deficits in ASD patients[37], the origins of these deficits are still largely unknown. Interestingly, one of the core diagnostic criteria for ASD includes

decrease eye-contact[38] and eye-tracking experiments have shown an impairment in orientation towards social stimuli in ASD patients [39]. Here, we propose that intact functionality of the SC – VTA^{DA} – DLS pathway may be fundamental for orientation towards conspecifics and deficits in this pathway may be upstream to social motivation dysfunctions in ASD patients.

In conclusion our data strongly suggest while SC – VTA^{DA} – DLS pathway encodes orientation towards an unfamiliar conspecific, AC – VTA^{DA} – NAc circuit function regulates the maintenance of social interaction. Elucidating the brain circuits underlying conspecific interaction is therefore essential, not only to understand how social behavior occurs, but also to comprehend the aberrant neural mechanisms underlying social deficits in psychiatric disorders.

References

1. Chen, P. & Hong, W. Neural Circuit Mechanisms of Social Behavior. *Neuron* **98,** 16–30 (2018).
2. Robinson, D. L., Heien, M. L. A. V. & Wightman, R. M. Frequency of dopamine concentration transients increases in dorsal and ventral striatum of male rats during introduction of conspecifics. *J. Neurosci.* **22,** 10477–10486 (2002).
3. Robinson, D. L., Zitzman, D. L., Smith, K. J. & Spear, L. P. Fast dopamine release events in the nucleus accumbens of early adolescent rats. *Neuroscience* **176,** 296–307 (2011).
4. Gunaydin, L. A. *et al.* Natural neural projection dynamics underlying social behavior. *Cell* **157,** 1535–1551 (2014).
5. Bariselli, S. *et al.* Role of VTA dopamine neurons and neuroligin 3 in sociability traits related to nonfamiliar conspecific interaction. *Nature Communications* **9,** 3173 (2018).
6. Freeman, A. S., Meltzer, L. T. & Bunney, B. S. Firing properties of substantia nigra dopaminergic neurons in freely moving rats. *Life Sciences* **36,** 1983–1994 (1985).
7. Guarraci, F. A. & Kapp, B. S. An electrophysiological characterization of ventral tegmental area dopaminergic neurons during differential pavlovian fear conditioning in the awake rabbit. *Behavioural Brain Research* **99,** 169–179 (1999).
8. Redgrave, P. & Gurney, K. The short-latency dopamine signal: a role in discovering novel actions? *Nat. Rev. Neurosci.* **7,** 967–975 (2006).
9. Dommett, E. *et al.* How visual stimuli activate dopaminergic neurons at short latency. *Science* **307,** 1476–1479 (2005).
10. May, P. J. *et al.* Tectonigral projections in the primate: a pathway for pre-attentive sensory input to midbrain dopaminergic neurons. *Eur. J. Neurosci.* **29,** 575–587 (2009).

11. Comoli, E. *et al.* A direct projection from superior colliculus to substantia nigra for detecting salient visual events. *Nature Neuroscience* **6,** 974–980 (2003).
12. McHaffie, J. G. *et al.* A direct projection from superior colliculus to substantia nigra pars compacta in the cat. *Neuroscience* **138,** 221–234 (2006).
13. Dean, P., Redgrave, P. & Westby, G. W. Event or emergency? Two response systems in the mammalian superior colliculus. *Trends Neurosci.* **12,** 137–147 (1989).
14. Dean, P., Pope, S. G. & Redgrave, P. Influence of novelty on locomotor hyperactivity after lesions of superior colliculus in rats. *Behavioural Brain Research* **5,** 213–218 (1982).
15. Comoli, E. *et al.* Segregated anatomical input to sub-regions of the rodent superior colliculus associated with approach and defense. *Front Neuroanat* **6,** 9 (2012).
16. Redgrave, P. *et al.* Interactions between the Midbrain Superior Colliculus and the Basal Ganglia. *Front Neuroanat* **4,** (2010).
17. Zhou, Z. *et al.* A VTA GABAergic Neural Circuit Mediates Visually Evoked Innate Defensive Responses. *Neuron* (2019). doi:10.1016/j.neuron.2019.05.027
18. Bromberg-Martin, E. S., Matsumoto, M. & Hikosaka, O. Dopamine in motivational control: rewarding, aversive, and alerting. *Neuron* **68,** 815–834 (2010).
19. Haber, S. N. The place of dopamine in the cortico-basal ganglia circuit. *Neuroscience* **282,** 248–257 (2014).
20. Beier, K. T. *et al.* Circuit Architecture of VTA Dopamine Neurons Revealed by Systematic Input-Output Mapping. *Cell* **162,** 622–634 (2015).
21. Watabe-Uchida, M. & Uchida, N. Multiple Dopamine Systems: Weal and Woe of Dopamine. *Cold Spring Harb. Symp. Quant. Biol.* 037648 (2019). doi:10.1101/sqb.2018.83.037648
22. Schultz, W. Dopamine reward prediction-error signalling: a two-component response. *Nature Publishing Group* **17,** 183–195 (2016).
23. Chevallier, C., Kohls, G., Troiani, V., Brodkin, E. S. & Schultz, R. T. The social motivation theory of autism. *Trends Cogn. Sci. (Regul. Ed.)* **16,** 231–239 (2012).
24. Jure, R. Autism Pathogenesis: The Superior Colliculus. *Front. Neurosci.* **12,** 1029 (2018).
25. Midgley, G. C., Wilkie, D. M. & Tees, R. C. Effects of superior colliculus lesions on rats' orienting and detection of neglected visual cues. *Behav. Neurosci.* **102,** 93–100 (1988).
26. Furigo, I. C. *et al.* The role of the superior colliculus in predatory hunting. *Neuroscience* **165,** 1–15 (2010).
27. Zingg, B. *et al.* AAV-Mediated Anterograde Transsynaptic Tagging: Mapping Corticocollicular Input-Defined Neural Pathways for Defense Behaviors. *Neuron* **93,** 33–47 (2017).
28. Evans, D. A. *et al.* A synaptic threshold mechanism for computing escape decisions. *Nature* **558,** 590–594 (2018).
29. Roeper, J. Dissecting the diversity of midbrain dopamine neurons. *Trends Neurosci.* **36,** 336–342 (2013).
30. Abercrombie, E. D., Keefe, K. A., DiFrischia, D. S. & Zigmond, M. J. Differential effect of stress on in vivo dopamine release in striatum, nucleus accumbens, and medial frontal cortex. *J. Neurochem.* **52,** 1655–1658 (1989).
31. Matsumoto, H., Tian, J., Uchida, N. & Watabe-Uchida, M. Midbrain dopamine neurons signal aversion in a reward-context-dependent manner. *eLife Sciences* **5,** 7025 (2016).
32. Brischoux, F., Chakraborty, S., Brierley, D. I. & Ungless, M. A. Phasic excitation of dopamine neurons in ventral VTA by noxious stimuli. *Proc. Natl. Acad. Sci. U.S.A.* **106,** 4894–4899 (2009).

33. Matsumoto, M. & Hikosaka, O. Two types of dopamine neuron distinctly convey positive and negative motivational signals. *Nature* **459,** 837–841 (2009).
34. Schultz, W., Tremblay, L. & Hollerman, J. R. Reward prediction in primate basal ganglia and frontal cortex. *Neuropharmacology* **37,** 421–429 (1998).
35. Cohen, J. Y., Haesler, S., Vong, L., Lowell, B. B. & Uchida, N. Neuron-type-specific signals for reward and punishment in the ventral tegmental area. *Nature* **482,** 85–88 (2012).
36. Takakuwa, N., Kato, R., Redgrave, P. & Isa, T. Emergence of visually-evoked reward expectation signals in dopamine neurons via the superior colliculus in V1 lesioned monkeys. *eLife Sciences* **6,** 10829 (2017).
37. Supekar, K. *et al.* Deficits in mesolimbic reward pathway underlie social interaction impairments in children with autism. *Brain* **141,** 2795–2805 (2018).
38. Falck-Ytter, T. & Hofsten, von, C. How special is social looking in ASD: a review. *Prog. Brain Res.* **189,** 209–222 (2011).
39. Franchini, M. *et al.* Social orienting and joint attention in preschoolers with autism spectrum disorders. *PLoS ONE* **12,** e0178859 (2017).

Acknowledgments: we are grateful to Lorena Jourdain for the technical support. We thank Manuel Mameli for the constructive comment on the manuscript and the entire Bellone lab for discussion.

Funding: This work was supported by funds to C.B from the Swiss National Science Foundation, NCCR SYNAPSY of the Swiss National Science Foundation, Fondation Von Meissner, Pierre Mercier and Fondation HUG.

Author Contribution: C.P.S. and A.C. performed behavioural tasks, virus injections and optic fiber cannulations. A.C. performed immunohistochemistry. S.B. and S.M. performed electrophysiological recordings. C.H. performed and analyzed with A.C. in vivo calcium recording. C.B. C.P.S. and A.C. designed the study. C.B. wrote the manuscript with the help of C.P.S. and A.C.

Competing interests: there are no competing interests

Data and material availability: All data is in the manuscript or in supplementary material. Videos will be made available on request.

Figure legends:

Figure 1: Anatomo-functional connectivity from SC to VTA DA neurons

(a) Schema of injection in the Superior Colliculus (SC) with the AAV5-hSyn-eYFP. **(b)** Representative coronal image of immuno-staining experiments against Tyrosine Hydroxylase (TH) enzyme (in red) performed on midbrain slices of adult mice infected with AAV5-hSyn-eYFP (green) in the SC. The projecting fibers from SC to VTA are visible. **(b')** Image at higher magnification of the coronal slice (scale bar: 100 µm). The fibers project from SC to VTA**. (c)** Schema of injection in the VTA with the CAV-Cre and with the AAV5-Ef1α-DIO-mCherry in the SC. **(d)** Left: Representative image of the infected cells with the CAV-Cre and AAV5-Ef1α-DIO-mCherry in the SC (scale bar: 200 µm). Right: schema reporting the position of mCherry positive cells in the SC for 4 infected brains. **(e)** Representative image of immuno-staining against Ca2+/calmodulin-dependent protein kinase II (CAMKII) in the SC and infected cells with the AAV5-Ef1α-DIO-mCherry (scale bar: 10 µm). **(f)** Quantification of infected cells in the SC. The cells are preferentially located in the intermediate layer of the SC. Quantification of infected cells co-localizing with CAMKII. The majority of the cells projecting to the VTA is positive for CAMKII and are then excitatory projections. **(g)** Schema of injection in the SC with AAV5-hSyn-ChR2-eYFP and patch of the VTA DA cells. **(h)** Whole cell patch clamp from SC infected neurons. Protocol of stimulation indicates that the cells of the SC follow the light stimulation protocol (20 Hz). **(i)** Example traces of optogenetically-induced excitatory post-synaptic current (oEPSC) or optogenetically-induced inhibitory post-synaptic current (oIPSC) in VTA DA neurons. **(j)** Quantification of connected cells from SC onto VTA DA neurons. The majority of connections are excitatory. Error bars report s.e.m.

Figure 2: Calcium activity of SC to VTA projecting cells during social interaction

(a) Schema of injections of AAVrg-Ef1α-mCherry-IRES-Cre in the VTA and AAV1/2-hSyn-FLEX-GCaMP6f-WPRE-SV40 in the SC. **(b)** Representative coronal image of midbrain slices of adult mice infected with AAVrg-Ef1α-mCherry-IRES-Cre in the VTA and AAV1/2-hSyn-FLEX-GCaMP6f-WPRE-SV40 in the SC. The site of the microendoscope is indicated (M). **(c) Up:** schema of the micro-endoscope Ca^{2+} imaging apparatus implanted in the SC. **Down:** example maximum intensity projection of image data of the GCaMP6f positive neurons in the SC projecting to the VTA. **(d)** Example of Ca^{2+} transients recorded from 7 SC neurons projecting to the VTA at basal condition (N = 1, scale bar: 50 µm). **(e)** Schema of

free social interaction and object exploration during Ca^{2+} imaging. Example of specific ensembles of cells exhibiting calcium responses during each session. The ensembles are highlighted with specific colors in the contour plots (N = 1). Colored contours were arbitrarily selected of some active neurons in each session (the firing rate is more than 0.5 [1/s] during each session). SC neurons projecting to the VTA are active for all conditions. **(f)** Cumulative distributions of Ca^{2+} transients dynamics of SC neurons projecting to the VTA during baseline conditions (before free social interaction and before object exploration), free social interaction and object exploration sessions (86 cells from N = 3). Kolmogorov-Smirnov two-samples test (Baseline 1 vs Social interaction: $Z = 2.439$, $P < 0.0001$; Baseline 2 vs Object exploration: $Z = 1.677$, $P = 0.0070$). **(g)** Percentage of active SC neurons projecting to the VTA during baseline conditions, free social interaction and object exploration. RM one-way ANOVA (Stimulus main effect: $F_{(1,83;\ 3.66)} = 11.66$ $P = 0.0260$) followed by Fisher post-hoc test. N indicates number of mice. Error bars report s.e.m.

Figure 3: SC – VTA pathway optogenetic manipulation alters social novelty approach

(a) Schema of injections sites in the SC with AAV5-hSyn-Jaws-eYFP or AAV5-hSyn-eYFP, and optic fiber implantation above the VTA. **(b)** Schema of injections sites in the SC with AAV5-hSyn-ChR2-eYFP or AAV5-hSyn-eYFP, and optic fiber implantation above the VTA. **(c)** Representative image of immuno-staining experiments against Tyrosine Hydroxylase (TH) enzyme (in red) performed on coronal midbrain slices of adult mice infected with AAV5-hSyn-ChR2-eYFP (green) in the SC. **(c')** Image at higher magnification of the VTA (scale bar: 100 µm). **(d)** Schema of free social interaction. The eYFP, Jaws-expressing and ChR2-expressing mice interact freely with two unfamiliar mice under both stimulation conditions. **(e)** Time social interaction during the free social interaction task for eYFP and Jaws mice. RM two-way ANOVA (Light main effect: $F_{(1,21)} = 2.7201$, $P = 0.1140$; Virus main effect: $F_{(1,21)} = 0.1985$, $P = 0.6605$; Light x Virus Interaction: : $F_{(1,21)} = 8.3378$, $P = 0.0088$) followed by Bonferroni-Holm post-hoc test correction. **(f)** Index of time social interaction to compare directly eYFP and Jaws mice. Unpaired t test ($t_{(21)} = -2.3266$). **(g)** Time social interaction during the free social interaction task for eYFP and ChR2 mice. RM two-way ANOVA (Light main effect: $F_{(1,28)} = 5.0855$, $P = 0.0321$; Virus main effect: $F_{(1,28)} = 0.8528$, $P = 0.3637$; Light x Virus Interaction: : $F_{(1,28)} = 4.1962$, $P = 0.0500$) followed by Bonferroni-Holm post-hoc test correction. **(h)** Index of time social interaction to compare directly eYFP and ChR2 mice. Unpaired t test ($t_{(28)} = 2.5267$). **(i)** Time following behavior for eYFP and Jaws-expressing mice under light-ON and light-OFF epochs. RM two-way

ANOVA (Light main effect: $F_{(1,21)} = 4.3333$, $P = 0.0498$; Virus main effect: $F_{(1,21)} = 0.9925$, $P = 0.3305$; Interaction Light x Virus: $F_{(1,21)} = 4.7701$, $P = 0.0404$) followed by Bonferroni-Holm post-hoc test correction. **(j)** Time nose-to-nose contact for eYFP and Jaws-expressing mice under light-ON and light-OFF epochs. RM two-way ANOVA (Light main effect: $F_{(1,21)} = 0.0198$, $P = 0.8895$; Virus main effect: $F_{(1,21)} = 0.0476$, $P = 0.8294$; Interaction Light x Virus: $F_{(1,21)} = 0.5243$, $P = 0.4770$) followed by Bonferroni-Holm post-hoc test correction. **(k)** Time grooming behavior during free social interaction task for eYFP and Jaws-expressing mice under light-ON and light-OFF epochs. RM two-way ANOVA (Light main effect: $F_{(1,21)} = 0.0792$, $P = 0.7812$; Virus main effect: $F_{(1,21)} = 8.3489$, $P = 0.0088$; Interaction Light x Virus: $F_{(1,21)} = 0.3857$, $P = 0.5413$). **(l)** Time rearing behavior during free social interaction task for eYFP and Jaws-expressing mice under light-ON and light-OFF epochs. RM two-way ANOVA (Light main effect: $F_{(1,21)} = 1.0594$, $P = 0.3151$; Virus main effect: $F_{(1,21)} = 1.3808$, $P = 0.2531$; Interaction Light x Virus: $F_{(1,21)} = 0.3329$, $P = 0.5701$). **(m)** Time following behavior for eYFP and ChR2-expressing mice under light-ON and light-OFF epochs. RM two-way ANOVA (Light main effect: $F_{(1,24)} = 3.1522$, $P = 0.0885$; Virus main effect: $F_{(1,24)} = 0.3289$, $P = 0.5716$; Interaction Light x Virus: $F_{(1,24)} = 2.7778$, $P = 0.1086$) followed by Bonferroni-Holm post-hoc test correction. **(n)** Time nose-to-nose contact for eYFP and ChR2-expressing mice under light-ON and light-OFF epochs. RM two-way ANOVA (Light main effect: $F_{(1,24)} = 0.0064$, $P = 0.9370$; Virus main effect: $F_{(1,24)} = 4.3794$, $P = 0.0471$; Interaction Light x Virus: $F_{(1,24)} = 6.4369$, $P = 0.0181$) followed by Bonferroni-Holm post-hoc test correction. **(o)** Time grooming behavior during free social interaction task for eYFP and ChR2-expressing mice under light-ON and light-OFF epochs. RM two-way ANOVA (Light main effect: $F_{(1,28)} = 0.0292$, $P = 0.8655$; Virus main effect: $F_{(1,28)} = 0.1635$, $P = 0.6890$; Interaction Light x Virus: $F_{(1,28)} = 0.3032$, $P = 0.5862$). **(p)** Time rearing behavior during free social interaction task for eYFP and ChR2-expressing mice under light-ON and light-OFF epochs. RM two-way ANOVA (Light main effect: $F_{(1,28)} = 0.3921$, $P = 0.5363$; Virus main effect: $F_{(1,28)} = 1.3238$, $P = 0.2596$; Interaction Light x Virus: $F_{(1,28)} = 0.5985$, $P = 0.4456$). Error bars report s.e.m.

Figure 4: SC – VTA pathway optogenetic manipulation alters head orientation towards conspecific

(a) Time course of the time social interaction for eYFP and Jaws mice in light and no-light stimulation conditions. RM two-way ANOVA (eYFP: Light main effect: $F_{(1,10)} = 0.4399$, $P = 0.5222$; Time main effect: $F_{(20,200)} = 7.902$, $P < 0.0001$; Light x Time Interaction: $F_{(20,200)} =$

0.5527, P = 0.9398. Jaws: Light main effect: $F_{(1,11)} = 7.188$, P = 0.0214; Time main effect: $F_{(20,220)} = 7.509$, P < 0.0001; Light x Time Interaction: $F_{(20,220)} = 0.6139$, P = 0.9005) followed by Bonferroni's multiple comparisons post-hoc test. Bonferroni's multiple comparisons post-hoc test significant values are labelled in yellow. **(b)** Time course of the time social interaction for eYFP and ChR2 mice in light and no-light stimulation conditions. RM two-way ANOVA (eYFP: Light main effect: $F_{(1,13)} = 0.01008$, P = 0.9216; Time main effect: $F_{(20,260)} = 13.52$, P < 0.0001; Light x Time Interaction: $F_{(20,260)} = 1.047$, P = 0.4074. ChR2: Light main effect: $F_{(1,15)} = 12.46$, P = 0.0030; Time main effect: $F_{(20,300)} = 10.35$, P < 0.0001; Light x Time Interaction: $F_{(20,300)} = 0.7968$, P = 0.7173) followed by Bonferroni's multiple comparisons post-hoc test. Bonferroni's multiple comparisons post-hoc test significant values are labelled in yellow. **(c)** Schema of head direction calculation for social stimulus. **(d)** Time course of the averaged angle between the eYFP and Jaws mice and the stimuli animals in light and no-light stimulation conditions. RM two-way ANOVA (eYFP: Light main effect: $F_{(1,10)} = 0.9762$, P = 0.3464; Time main effect: $F_{(19,190)} = 2.349$, P = 0.0019; Light x Time Interaction: $F_{(19,190)} = 0.3207$, P = 0.9972. Jaws: Light main effect: $F_{(1,11)} = 3.998$, P = 0.0709; Time main effect: $F_{(19,209)} = 1.853$, P = 0.0192; Light x Time Interaction: $F_{(19,209)} = 1.14$, P = 0.3136) followed by Bonferroni's multiple comparisons post-hoc test. Bonferroni's multiple comparisons post-hoc test significant values are labelled in yellow. **(e)** Time course of the averaged angle between the eYFP and ChR2 mice and the stimuli animals in light and no-light stimulation conditions. RM two-way ANOVA (eYFP: Light main effect: $F_{(1,13)} = 0.7902$, P = 0.3902; Time main effect: $F_{(20,260)} = 5.513$, P < 0.0001; Light x Time Interaction: $F_{(20,260)} = 0.8264$, P = 0.6806. ChR2: Light main effect: $F_{(1,15)} = 10.38$, P = 0.0067; Time main effect: $F_{(20,300)} = 4.838$, P < 0.0001; Light x Time Interaction: $F_{(20,300)} = 0.2049$, P = 0.0060) followed by Bonferroni's multiple comparisons post-hoc test. Bonferroni's multiple comparisons post-hoc test significant values are labelled in yellow. **(f)** Linear regressions between the mean head-oriented angle and the mean time of interaction per time-bin = 10 seconds across the free interaction session for eYFP- and Jaws-expressing mice (light OFF and light ON epochs). The time across the free interaction session is indicated by the colour of the point (colour-scale on the lower right angle of each graph). **(g)** Linear regressions between the mean head-oriented angle and the mean time of interaction per time-bin = 10 seconds across the free interaction session for eYFP- and ChR2-expressing mice (light OFF and light ON epochs). The time across the free interaction session is indicated by the colour of the point (colour-scale on the lower right angle of each graph). **(h)** Cumulative probability of the head direction depending on the angle made with the

conspecific. RM two-way ANOVA (eYFP: Light main effect: $F_{(1,10)} = 0.7565$, $P = 0.4048$; Angle main effect: $F_{(17,170)} = 680.2$, $P < 0.0001$; Light x Angle Interaction: $F_{(17,170)} = 1.429$, $P = 0.1284$. Jaws: Light main effect: $F_{(1,11)} = 5.026$, $P = 0.0465$; Angle main effect: $F_{(17,187)} = 687$, $P < 0.0001$; Light x Angle Interaction: $F_{(17,187)} = 3.782$, $P < 0.0001$) followed by Bonferroni's multiple comparisons post-hoc test. Bonferroni's multiple comparisons post-hoc test significant values are labelled in yellow. **(i)** Cumulative probability of the head direction depending on the angle made with the conspecific. RM two-way ANOVA (eYFP: Light main effect: $F_{(1,13)} = 1.34$, $P = 0.2679$; Angle main effect: $F_{(17,221)} = 1220$, $P < 0.0001$; Light x Angle Interaction: $F_{(17,221)} = 0.8888$, $P = 0.5879$. ChR2: Light main effect: $F_{(1,13)} = 3.986$, $P = 0.0673$; Angle main effect: $F_{(17,221)} = 1248$, $P < 0.0001$; Light x Angle Interaction: $F_{(17,221)} = 4.397$, $P < 0.0001$) followed by Bonferroni's multiple comparisons post-hoc test. Bonferroni's multiple comparisons post-hoc test significant values are labelled in yellow. N indicates number of mice. # indicates significantly different interaction. Error bars report s.e.m.

Figure 5: Stimulation of AC – VTA pathway increase social interaction

(a) Schema of injection in Anterior Cortex (AC) and optic fiber implantation above the VTA. **(b)** Representative image of injection site in the anterior cortex (mAC: medial anterior cortex, lAC: lateral injection cortex). Adult mice brains were infected with AAV5-hSyn-ChR2-eYFP (green) (scale bar: 500 µm). (**c**) Representative image of immuno-staining experiments against Tyrosine Hydroxylase (TH) enzyme (in red) performed on coronal midbrain slices of adult mice infected with AAV5-hSyn-ChR2-eYFP (green) in the AC and implanted in the VTA with a optic fiber. **(c')** Image at higher magnification of the VTA with fibers from the AC and the optic fiber's track (scale bar: 100 µm). **(d)** Schema of free social interaction. The mice interact freely with two unfamiliar mice under both stimulation conditions. **(e)** Time of social interaction in the free interaction task for eYFP and ChR2 mice in both stimulation conditions. RM two-way ANOVA (Light main effect: $F_{(1,25)} = 7.1991$, $P = 0.0127$; Virus main effect: $F_{(1,25)} = 2.6938$, $P = 0.1133$; Interaction Light x Virus: $F_{(1,25)} = 2.4605$, $P = 0.1293$) followed by Bonferroni-Holm post-hoc test correction. **(f)** Time course of the time social interaction for AC-eYFP and -ChR2 mice in light and no-light stimulation conditions. RM two-way ANOVA (eYFP: Light main effect: $F_{(1,12)} = 0.4209$, $P = 0.5287$; Time main effect: $F_{(20,240)} = 6.134$, $P < 0.0001$; Light x Time Interaction: $F_{(20,240)} = 0.8283$, $P = 0.6780$. ChR2: Light main effect: $F_{(1,13)} = 11.77$, $P = 0.0045$; Time main effect: $F_{(20,260)} = 10.49$, $P < 0.0001$; Light x Time Interaction: $F_{(20,260)} = 0.9466$, $P = 0.5284$) followed by Bonferroni's

multiple comparisons post-hoc test. **(g)** Cumulative probability of the head direction depending the angle made with the conspecific. Left: eYFP mice: RM two-way ANOVA (Light main effect: $F_{(1,12)} = 0.002477$, $P = 0.9611$; Angle main effect: $F_{(17,204)} = 1346$, $P < 0.0001$; Light x Angle Interaction: $F_{(17,204)} = 0.3352$, $P = 0.9943$). Right, ChR2 mice: RM two-way ANOVA (Light main effect: $F_{(1,15)} = 0.0015$, $P = 0.9693$; Angle main effect: $F_{(17,255)} = 613.5$, $P < 0.0001$; Light x Angle Interaction: $F_{(17,255)} = 4.397$, $P = 0.7354$). N indicates number of mice. Error bars report s.e.m.

Figure 6: SC – VTA DA connected neurons project to DLS. Stimulation of VTA DA – DLS pathway induces similar social interaction alterations

(a) Schema of injection of CTB 488 and CTB 555 respectively in the NAc and DLS. **(b)** Representative image of the NAc and DLS in coronal slice infected with the CTB 488 and CTB 555. **(c)** Coronal image of the VTA with TH staining and infected cells projecting to the NAc or DLS. **(d)** Infected cells of the VTA with the CTB 488 and CTB 555 in horizontal plan. **(e)** Schema of proportion of TH^+ and either $TH^+/CTB488^+$ (NAc-projecting VTA DA neurons) or $TH^+/CTB555^+$ (DLS-projecting VTA DA neurons). **(f)** Schema of injection in the SC with the AAV5-hSyn-ChR2-eYFP (Right) and in the Tail Striatum, the Nucleus Accumbens or the Dorso-Lateral Striatum (Left) with the AAVrg-pCAG-FLEX-tdTomato in DAT-Cre mice, to patch DA neurons receiving SC projections and projecting to different specific regions. **(g)** Quantification of SC – VTA DA connected cells projecting to the TS, the DLS or the NAc. The VTA DA neurons receiving projections from the SC are mainly projecting to the DLS with the highest current amplitude. **(h)** Left: Schema of injections sites in the VTA of DAT-Cre mice with AAV5-Ef1α-DIO-eYFP or AAV5-Ef1α-DIO-ChR2-eYFP, and optic fiber implantation above the dorsal striatum (DS). Middle: representative image showing the fiber optic's track in the DS. Right: representative image of site of injection in the VTA. (**i**) Left: Schema of injections sites in the VTA of DAT-Cre mice with AAV5-Ef1α-DIO-ChR2-eYFP or AAV5-Ef1α-DIO-eYFP, and optic fiber implantation above the nucleus accumbens (NAc). Middle: representative image showing the fiber optic's track in the NAc. Right: representative image of site of injection in the VTA. (**j**) Schema of free social interaction. The mice interact freely with two unfamiliar mice under both stimulation conditions: photo-stimulation of the pathway VTA^{DA} – NAc or VTA^{DA} – DLS. **(k)** $VTA^{DA}::NAc^{eYFP}$ / $VTA^{DA}::DLS^{eYFP}$ mice do not change time of social interaction between the two stimulation conditions. Paired t test ($t_{(11)} = -0.4866$). **(l)** $VTA^{DA}::NAc^{ChR2}$ mice increase the time of social interaction when the pathway VTA^{DA} – NAc is

optogenetically stimulated. Paired t test ($t_{(11)}$ = -2.8177). **(m)** VTA^{DA}::DLS^{ChR2} mice decrease the time of social interaction when the pathway VTA^{DA} – DLS is optogenetically stimulated. Paired t test ($t_{(11)}$ = -2.7696). **(n)** Index of time social interaction when photo-stimulating the VTA^{DA} to NAc or DLS pathways. Mice increase social interaction for the NAc pathway while they decrease the social interaction for the DLS pathway. One-way ANOVA (Group main effect: $F_{(2, 33)}$ = 6.56, P = 0.0040) followed by one-sample t test Bonferroni-Holm corrected. Error bars report s.e.m.

Supplementary figure 1: SC – VTA pathway optogenetic manipulation does not alter free object exploration

(a) Schema of free object interaction. The mice interact freely with two novel objects under both light conditions. **(b)** Time object interaction during the free object interaction task for eYFP and Jaws-expressing mice. RM two-way ANOVA (Light main effect: $F_{(1,47)}$ = 0.1281, P = 0.7238; Virus main effect: $F_{(1,47)}$ = 0.1624, P = 0.6908; Light x Virus Interaction: : $F_{(1,47)}$ = 1.3539, P = 0.2571). **(c)** Time object interaction during the free object interaction task for eYFP and ChR2-expressing mice. RM two-way ANOVA (Light main effect: $F_{(1,50)}$ = 0.01269, P = 0.8775; Virus main effect: $F_{(1,50)}$ = 1.791, P = 0.1869; Light x Virus Interaction: : $F_{(1,50)}$ = 0.5158, P = 0.4760). **(d)** Schema of head direction calculation for inanimate object stimulus. **(e)** Cumulative probability of the head direction depending the angle made with the object stimulus. eYFP: RM two-way ANOVA (Light main effect: $F_{(1,10)}$ = 1.203, P = 0.2985; Angle main effect: $F_{(17,170)}$ = 345.9, P < 0.0001; Light x Angle Interaction: $F_{(17,170)}$ = 0.7302, P = 0.7689). Jaws: RM two-way ANOVA (Light main effect: $F_{(1,11)}$ = 0.5069, P = 0.4913; Angle main effect: $F_{(17,187)}$ = 307.1, P < 0.0001; Light x Angle Interaction: $F_{(17,187)}$ = 0.8884, P = 0.5884) followed by Bonferroni post-hoc test correction. **(f)** Cumulative probability of the head direction depending the angle made with the object stimulus. eYFP: RM two-way ANOVA (Light main effect: $F_{(1,12)}$ = 0.4095, P = 0.5343; Angle main effect: $F_{(17,204)}$ = 331.9, P < 0.0001; Light x Angle Interaction: $F_{(17,204)}$ = 0.377, P = 0.9888). ChR2: RM two-way ANOVA (Light main effect: $F_{(1,13)}$ = 5.149, P = 0.0409; Angle main effect: $F_{(17,221)}$ = 455.9, P < 0.0001; Light x Angle Interaction: $F_{(17,221)}$ = 3.955, P < 0.0001) followed by Bonferroni post-hoc test correction. N indicates number of mice. # indicates significantly different interaction. Error bars report s.e.m.

Supplementary figure 2: SC – VTA pathway stimulation alters social preference and social novelty exploration

(a) Schema of the 3-chamber task. The mice undergo habituation, social preference and social novelty phases, in light and no-light stimulation conditions. **(b)** Time sniffing the object and the conspecific sex-matched under light and no-light stimulation conditions for eYFP and ChR2 mice. eYFP mice: RM two-way ANOVA (Stimulus main effect: $F_{(1,18)}$ = 50.5803, P < 0.0001; Light main effect: $F_{(1,18)}$ = 1.3108, P = 0.2673; Interaction Stimulus x Light: $F_{(1,18)}$ = 0.0799, P = 0.7806) followed by Bonferroni-Holm post-hoc test correction. ChR2 mice: RM two-way ANOVA (Stimulus main effect: $F_{(1,16)}$ = 19.7522, P < 0.0004; Light main effect: $F_{(1,16)}$ = 0.1378, P = 0.7154; Interaction Stimulus x Light: $F_{(1,16)}$ = 3.8880, P = 0.0662) followed by Bonferroni-Holm post-hoc test correction. **(c)** Time sniffing the familiar and unfamiliar conspecific under light and no-light stimulation conditions for eYFP and ChR2 mice. eYFP mice: RM two-way ANOVA (Stimulus main effect: $F_{(1,18)}$ = 66.8642, P < 0.0001; Light main effect: $F_{(1,18)}$ = 0.5532, P = 0.4666; Interaction Stimulus x Light: $F_{(1,18)}$ = 0.0002, P = 0.9881) followed by Bonferroni-Holm post-hoc test correction. ChR2 mice: RM two-way ANOVA (Stimulus main effect: $F_{(1,16)}$ = 17.9956, P < 0.0006; Light main effect: $F_{(1,16)}$ = 0.4732, P = 0.5010; Interaction Stimulus x Light: $F_{(1,16)}$ = 49.1223, P < 0.0001) followed by Bonferroni-Holm post-hoc test correction. **(d)** Schema of long-term social habituation/novelty exploration task. The animals undergo photo-stimulation protocol the 5th day during social novelty exploration. **(e)** Time social interaction in the long-term social habituation/novelty task for eYFP and ChR2 mice in light and no-light stimulation conditions (day 4 and day 5). RM two-way ANOVA (Light main effect: $F_{(1,31)}$ = 2.4057, P = 0.1310; Virus main effect: $F_{(1,31)}$ = 0.0216, P = 0.8840; Light x Virus Interaction: $F_{(1,31)}$ = 2.0668, P = 0.0003) followed by Bonferroni-Holm post-hoc test correction. **(f)** Index of time social interaction to compare directly eYFP and ChR2 mice. Unpaired t test ($t_{(31)}$ = 3.7864). N indicates number of mice. # indicates significantly different interaction. Error bars report s.e.m.

Supplementary figure 3: SC – VTA stimulation does not affect familiar conspecific interaction.

(a) Schema of free social interaction. The mice interact freely with one mouse twice first without photostimulation (T1) then during light-ON epoch (T2). **(b)** Time spent in social interaction with the conspecific during T1 and T2 for eYFP- and Jaws-expressing mice. RM two-way ANOVA (Light main effect: $F_{(1,20)}$ = 26.1519, P = 0.0001; Virus main effect: $F_{(1,20)}$ = 0.0672, P = 0.7982; Interaction Light x Virus: $F_{(1,20)}$ = 0.0970, P = 0.7586) followed by Bonferroni-Holm post-hoc test correction. **(c)** Index of time social interaction to compare

directly eYFP and Jaws-expressing mice. Mann-Whitney test (U = 126). **(d)** Time spent in social interaction with the conspecific during T1 and T2 for eYFP-control and ChR2-expressing mice. RM two-way ANOVA (Light main effect: $F_{(1,12)} = 20.7890$, P = 0.0007; Virus main effect: $F_{(1,12)} = 1.1988$, P = 0.2950; Interaction Light x Virus: $F_{(1,25)} = 0.8072$, P = 0.3866) followed by Bonferroni-Holm post-hoc test correction. **(e)** Index of time social interaction to compare directly eYFP and ChR2-expressing mice. Unpaired t test ($t_{(12)} = 0.1718$). Error bars report s.e.m.

Supplementary figure 4: SC – VTA pathway stimulation is not reinforcing per se

(a) Schema of the open-field arena. The mice are free to explore the apparatus during 10 mins in both stimulations conditions. **(b)** Tracking examples for eYFP and Jaws mice in light and no-light stimulation conditions. **(c-d)** Distance moved in the open-field arena for eYFP and Jaws mice under light and no-light stimulation. RM two-way ANOVA (Light main effect: $F_{(1,21)} = 0.0046$, P = 0.9466; Virus main effect: $F_{(1,21)} = 0.1789$, P = 0.6766; Light x Virus interaction: $F_{(1,21)} = 0.7033$, P = 0.4111). **(e)** Tracking examples for eYFP and ChR2 mice in light and no-light stimulation conditions. **(f-g)** Distance moved in the open-field arena for eYFP and ChR2 mice under light and no-light stimulation. RM two-way ANOVA (Light main effect: $F_{(1,18)} = 4.0046$, P = 0.0607; Virus main effect: $F_{(1,18)} = 4.8210$, P = 0.0415; Light x Virus interaction: $F_{(1,18)} = 4.8217$, P = 0.0415) followed by Bonferroni-Holm post-hoc test correction. **(h)** Schema of open field arena divided between periphery and center. **(i)** Time passed in the center of the open-field arena for eYFP and Jaws mice under light and no-light stimulation. RM two-way ANOVA (Light main effect: $F_{(1,21)} = 0.4212$, P = 0.5234; Virus main effect: $F_{(1,21)} = 0.5217$, P = 0.4781; Light x Virus interaction: $F_{(1,21)} = 0.02339$, P = 0.8799). **(j)** Time passed in the center of the open-field arena for eYFP and ChR2 mice under light and no-light stimulation. RM two-way ANOVA (Light main effect: $F_{(1,18)} = 0.1628$, P = 0.6913; Virus main effect: $F_{(1,18)} = 0.145$, P = 0.7078; Light x Virus interaction: $F_{(1,18)} = 0.546$, P = 0.4695). **(k)** Schema of the real-time place preference set up. The optogenetic stimulation is assigned to one chamber while the other is not associated with any stimulation. The mice are free to explore the apparatus during 10 mins. **(l)** Time spent in the chamber associated with the photostimulation or not for eYFP and Jaws mice. RM two-way ANOVA (Light main effect: $F_{(1,16)} = 0.9683$, P = 0.3398; Virus main effect: $F_{(1,16)} = 0.2699$, P = 0.6105; Light x Virus Interaction: $F_{(1,16)} = 0.5421$, P = 0.4722). **(m)** Time spent in the chamber associated with the photostimulation or not for eYFP and ChR2 mice. RM two-way ANOVA (Light main effect: $F_{(1,29)} = 4.3617$, P = 0.0456; Virus main effect: $F_{(1,29)} = 5.2176$,

824 P = 0.0299; Light x Virus Interaction: $F_{(1,29)} = 0.7305$, P = 0.3997) followed by Bonferroni-
825 Holm post-hoc test correction. N indicates number of mice. # indicates significantly different
826 interaction. Error bars report s.e.m.
827
828

Material and Methods

Mice

Male wild type (WT; C57Bl/6J) and DAT-iresCre (Slc6a3$^{tm1.1(cre)Bkmn}$/J, called DAT-Cre in the rest of manuscript) were employed for this study. Mice were housed in groups (weaning at P21 – P23) under a 12 hours light – dark cycle (7:00 a.m.–7:00 p.m.) with food and water ad libidum. All physiology and behavior experiments were performed during the light cycle (the experiments were performed in a time window that started approximately 2 h after the end of the dark circle and ended 2 h before the start of the next dark circle) and were conducted in a room with fixed illumination (20 Lux) at a temperature between 22°C and 24°C.All the procedures performed at UNIGE complied with the Swiss National Institutional Guidelines on Animal Experimentation and were approved by the respective Swiss Cantonal Veterinary Office Committees for Animal Experimentation.

Stereotaxic injection

rAAV5-hSyn-hChR2(H134R)-eYFP, rAAV5-hSyn-Jaws-KGC-GFP-ER2 or rAAV5-hSyn-eYFP were injected in WT mice at 4 – 7 weeks. Mice were anesthetized with a mixture of oxygen (1 L/min) and isoflurane 3% (Baxter AG, Vienna, Austria) and placed in a stereotactic frame (Angle One; Leica, Germany). The skin was shaved, locally anesthetized with 40–50 µL lidocaine 0.5% and disinfected. The animals were placed in a stereotactic frame and bilateral craniotomy was made over the Superior Colliculus (SC) at the following stereotactic coordinates: ML ± 0.8 mm, AP -3.4 mm, DV −1.5 mm from Bregma, for a total volume of 500 nL for each side. For the Anterior Cortex (AC), bilateral injections were performed, at 4 different sites, at the following coordinates: ML ± 2.2 mm, AP +2.1 mm, DV −2.1 mm from Bregma, 300 nL each side, and ML ± 0.3 mm, AP +1.95 mm, DV −2.1 mm, 200 nL each side. The virus was injected via a glass micropipette (Drummond Scientific Company, Broomall, PA). Injections sites were confirmed post hoc by immunostaining on SC. The virus was incubated for 3 – 4 weeks and subsequently mice were implanted with optic fibers above the VTA. The animals were anesthetized, placed in a stereotactic frame, the skin was shaved and a unilateral craniotomy was performed as previously described. The optic fiber was implanted with a 10° angle at the following coordinates: ML ± 0.9 mm, AP −3.2 mm, DV −3.95 ± 0.05 mm from Bregma above the VTA and fixed to the skull with dental acrylic.

For optogenetic experiments using DAT-Cre mice, the animals were injected with rAAV5-Ef1α-DIO-hChR2(H134R)-eYFP or rAAV5-Ef1α-DIO-eYFP in the VTA. The animals were anesthetized, placed in a stereotactic frame, the skin was shaved and bilateral craniotomies were performed as previously described. The virus was incubated for 3 – 4 weeks and subsequently mice were implanted with optic fibers above either the Nucleus Accumbens (NAc) with 15° angle at the following coordinates: ML ± 2.0 mm, AP +1.2 mm, DV −4.2 mm from Bregma ;or the dorsolateral Striatum (DLS) at the following coordinates: ML ± 2.0 mm, AP +1.0 mm, DV −2.5 mm from Bregma. The optic fibers were then fixed using dental acrylic. Optic fibers placement was finally confirmed post-hoc by slicing the brain and taking pictures to the microscope.

For *ex-vivo* electrophysiological recording experiments, injections of retrograde AAVrg-pCAG-FLEX-tdTomato-WPRE and rAAV5-hSyn-hChR2(H134R)-eYFP were performed in DAT-Cre mice. The animals were anesthetized, placed in a stereotactic frame, the skin was shaved and bilateral craniotomies were performed as previously described. rAAV5-hSyn-hChR2(H134R)-eYFP was first injected in the SC at the same coordinates previously described and then the AAVrg-pCAG-FLEX-TdTomato was bilateraly injected either in the NAc at these coordinates: ML ± 1.0 mm, AP +1.2 mm, DV −4.4 / −4.0 mm from Bregma, 500 nL each side; either the DLS at following coordinates: ML ± 2.0 mm, AP +1.0 mm, DV −2.8 mm from Bregma, 500 nL each side; or the tail of the Striatum (TS) at these coordinates: ML ± 3.2 mm, AP −1.75 mm, DV −2.1 mm from Bregma, 500 nL each side. The viruses were incubated 3 – 4 weeks before to perform *ex-vivo* electrophysiological recordings. rAAV5-hSyn-hChR2(H134R)-eYFP was also injected in the SC in WT mice as described above at the same coordinates.

For anatomical validation experiments, bilateral injections of rAAV5-hSyn-eYFP in the SC were performed as described above. The virus was incubated 3 – 4 weeks before immunostaining procedures. CAV-2 Cre and rAAV5-hSyn-DIO-mCherry were injected in WT mice. The mice underwent the same surgical procedure, as described above, and the CAV-2 Cre was bilaterally injected in the VTA at the following coordinates: ML ± 0.5 mm, AP −3.2 mm, DV −4.20 ± 0.05 mm from Bregma, 500 nL each side. Then the rAAV5-hSyn-DIO-mCherry was bilaterally injected in the SC at the same coordinates described previously. The viruses were incubated 3 – 4 weeks prior immunostaining experiments.

Finally, WT mice were bilaterally injected using Cholera Toxin subunit-B Alexa fluor 555 (CTB 555) or CTB 488 respectively in the DLS (ML ± 2.0 mm, AP +1.0 mm, DV −2.8 mm from Bregma, 200 nL each side) and the NAc (ML ± 1.0 mm, AP +1.2 mm, DV −4.4 / −4.0

mm from Bregma, 200 nL each side). The CTB 488 and CTB 555 were incubated during 2 weeks before immunostaining procedures.

GRIN lens implantation for Calcium imaging: AAVrg-Ef1α-mCherry-IRES-Cre was injected in the VTA (see coordinates above) and AAV1/2-hSyn-FLEX-GCaMP6f-WPRE-SV40 was injected in the SC (see coordinates above) in WT mice at 4 – 7 weeks. As described above, animals were anesthetized the skin was shaved and bilateral craniotomy was performed over the VTA and the SC. The viruses were incubated 3 – 4 weeks prior immunostaining experiments.

3 weeks after, a 0.5 mm diameter GRIN snap-in imaging cannula (Model D, Doric lenses Inc., Canada) was implanted above the SC. After anaesthesia and craniotomy, the GRIN lens was slowly lowered in the brain by ~1.35-1.45 mm in DV (AP and ML are the same than the stereotaxic injection) from brain surface and until previously injected GCaMP6f signals were observed using a snap-in fluorescence microscope body (Doric lenses Inc.). After finding a suitable imaging site (~100 µm above the target neuronal population), the GRIN cannula was secured to the skull using cyanoacrylic glue and dental cement. A custom-made head post was also firmly attached to the skull with cyanoacrylic glue and dental cement. All mice were allowed to recover for more than three weeks after surgery and were then habituated to a snap-in fluorescence microscope body (OSFM, Doric lenses Inc., Canada) attachment and *in-vivo* imaging for more than five days before any behavioural experiments.

Direct interaction

An experimental cage similar to the animal's homecage was used for this task. The bedding was replaced after each trial. All eYFP-control, Jaws and ChR2-expressing mice (male C57Bl/6J; group-housed; 8 – 14 weeks) underwent both conditions of light-ON or light-OFF epochs. For eYFP-control and ChR2-expressing mice, the following optogenetic stimulation protocol was used: burst of 8 pulses of 4 msec light at 30 Hz every 5 sec (Imetronic, Pessac, France), wavelength of 488 nm (BioRay Laser, Coherent). For eYFP-control and Jaws-expressing mice, a constant light-ON epoch was delivered (Imetronic, Pessac, France), at 647 nm wavelength (BioRay Laser, Coherent). The experimental mice were first placed in the cage for 3 mins to explore freely the new environment. The light stimulation or inhibition protocols were applied or not depending the random assignment to the batch. After 3 mins, a social stimulus (unfamiliar juvenile conspecific sex-matched C57BL/6J, 3 – 4 weeks; s1) was introduced in the cage, and the animals were free to interact during 2 mins. The mice were then removed and placed in their respective cages. After 3 hours, the same experimental

design was performed and the mice that received the light stimulation or inhibition protocols did not receive it and *vice versa*. Another unfamiliar conspecific stimulus (s2) was introduced for 2 mins in the cage after the 3 mins of exploration. At the end, all the animals underwent both optical stimulation conditions (light-ON or light-OFF epochs). The same protocol, as described above, was used for the free object interaction task using 2 different unfamiliar inanimate object stimuli (o1 and o2), for eYFP-control, Jaws and ChR2-expressing mice.

During the free social interaction task, nonaggressive interaction was scored (experimenter blind to the viral injection and optical protocol) when the experimental mouse initiated the action and when the nose of the animal was oriented towards the conspecific only. The time social interaction was used to calculate the Index Time Social interaction as: $\frac{Social\ Interaction^{Light}}{Social\ Interaction^{Light} + Social\ Interaction^{No_Light}}$. During the free object interaction task, the interaction was scored when the nose of the animal was oriented towards the object stimulus. The time object interaction was used to calculate the Index Time Object interaction as: $\frac{Object\ Interaction^{Light}}{Object\ Interaction^{Light} + Object\ Interaction^{No_Light}}$.

Every session was video-tracked and recorded using Ethovision XT (Noldus, Wageningen, the Netherlands). Using the vector formed by the gravity center and the nose of the experimental mice, it has been possible to manually calculate the head orientation, depending different angles, towards the gravity center of the conspecific stimulus. Since the inanimate object is fixed, the head direction was automatically computed by EthoVision software taking radius angle (defined by a circle of 5 cm around the object).

Mice injected with rAAV5-hSyn-eYFP or rAAV5-hSyn-hChR2(H134R)-eYFP in Anterior Cortex (AC) and implanted with optic fiber in the VTA performed the free social interaction task with the same optical stimulation (burst of 8 pulses of 4 msec light at 30 Hz every 5sec; Imetronic, Pessac, France) and behavioral protocols.

Likewise, DAT-Cre mice injected with rAAV5-Ef1α-DIO-eYFP or rAAV5-Ef1α-DIO-hChR2(H134R)-eYFP in the VTA and implanted with double optic fiber either in the Nucleus Accumbens (VTA^{DA}::NAc^{eYFP} or VTA^{DA}::NAc^{ChR2}) or dorsolateral Striatum (VTA^{DA}::DLS^{eYFP} or VTA^{DA}::DLS^{ChR2}) underwent the same protocol of free social interaction task as described above. The behavior was scored and the Index Time Social interaction was calculated as explained previously.

The power expected at the tip of the optic fiber was between 8 – 12 mW. To this aim the laser power was checked before every experiment and the power at the optic fiber tip was controlled before any implantation.

After the task, the animals were sacrificed and the viral infection was verified. If no infection was detected or the optic fiber not in the right area, the mice were excluded from the batch. The apparatus was cleaned using 70% ethanol after each session.

Direct interaction for *in-vivo* calcium imaging

Mice injected with AAVrg-Ef1α-mCherry-IRES-Cre in the VTA and AAV1/2-hSyn-FLEX-GCaMP6f-WPRE-SV40 and implanted with SNAP-in GRIN cannula in the SC performed both the free social interaction task and the object exploration task with monitoring the Ca^{2+} dynamics. The first day the experimental mice performed the free social interaction task and the following day the experimental mice performed the object exploration task. The experimental mice were first placed in a cage like-home cage for 5 mins to explore freely the new environment. Subsequently the exploring session, a social stimulus for the free social interaction and a locker (40 mm x 15 mm x 60 mm) for object exploration task was introduced in the cage and the animals were free to interact during 5 mins. At the end, the experimental mouse is placed back in its homecage. The stimulus mouse for the free social interaction, and the object for the free object exploration task are removed from the experimental cage. After the task, the animals were sacrificed and the viral infection was verified. If no infection was detected or the microendoscope not in the right area, the mice were excluded from the batch. The apparatus was cleaned using 70% ethanol after each session.

Three chamber interaction task

The three-chambered social preference test was performed in a rectangular Plexiglas arena (60 × 40 × 22 cm) (Ugo Basile, Varese, Italy) divided into three chambers (each 20 × 40 × 22 cm) that communicate by removable doors situated on the walls of the center chamber. One week after optic fiber implantation, eYFP-control and ChR2-expressing mice were randomly assigned to two batches that received the optical stimulation protocol or not (burst of 8 pulses of 4ms light at 30Hz every 5sec; Imetronic, Pessac, France). One to two weeks after, the experimental subjects that underwent first the optogenetic stimulation did not receive any light-stimulation and *vice versa*, thus performing the task in both conditions. The habituation phase consisted in 10 min of free exploration of the empty arena. The habituation was always done in no-light epoch. Subsequently, the mouse was temporarily kept in the center chamber by closing the removable doors. Two enclosures were placed in the centers of the side chambers. One enclosure was left empty (inanimate object) and the other one contained an

unfamiliar conspecific stimulus (unfamiliar juvenile mice C57BL/6J, 3 – 4 weeks). The light stimulation protocol was applied to the associated batch. The doors were then removed and the experimental mouse freely explored the arena and the two enclosures for 10 min. The walls of the enclosures, consisting of vertical metal bars, allowed visual, auditory, olfactory and tactile contact between the experimental mouse and the stimulus mouse. The position of the stimuli was randomly assigned and counterbalanced. The mice were then restrained a second time in the center chamber by closing the removable doors. The enclosures were held in position and an unfamiliar conspecific was placed in the empty one. In this phase, the prior unfamiliar conspecific is considered as familiar (social familiar). The light stimulation was applied again for the mice that received it during the social preference phase. The doors were opened and the experimental mouse explored the arena for 10 min, with the two enclosures containing the familiar and the unfamiliar conspecific stimuli. At the end of the 10 min, the experimental and stimuli mice returned to their home cage. Every session was video-tracked and recorded using Ethovision XT (Noldus, Wageningen, the Netherlands), which provided the time in the different chambers and the distance moved during the test. An experimenter blind to the viral infection of animals also manually scored behavior. The stimulus interaction was scored when the nose of the experimental subject was oriented towards the enclosures at a distance approximately less than 2 cm. After the task, the animals were sacrificed and the viral infection was verified. The optic fiber integrity was checked again by controlling the light power. If no infection was noticed or the optic fiber not in the right area, the mice were excluded from the batch. The apparatus was cleaned using 70% ethanol after each session.

Open Field

Mice injected with rAAV5-hSyn-eYFP, rAAV5-hSyn-Jaws-KGC-GFP-ER2 or rAAV5-hSyn-hChR2(H134R)-eYFP in Superior Colliculus (SC) and implanted with optic fiber in the VTA performed the open-field task (OF). The eYFP-control, Jaws and ChR2-expressing mice were placed in the OF arena for 10 min. The apparatus consisted in a 40 cm sided Plexiglas squared arena. The mice were randomly assigned to the optical light stimulation/ inhibition protocols (as previously described) or not (Imetronic system, Pessac, France). After 10 min of free exploration the mice were placed back into their homecage. 3 hours later the animals were re-tested in the OF experiment and the mice that received the light-ON epoch did not receive it and *vice versa*. At the end, all the animals performed both conditions. The OF task was video-tracked (Ethovision, Noldus, Wageningen, the Netherlands) to automatically obtain the distance moved. After the task, the animals were

sacrificed and the viral infection was verified. If no infection was noticed or the optic fiber not in the right area, the mice were excluded from the batch. The apparatus was cleaned using 70% ethanol after each session.

Real Time Place Preference task

WT mice injected with rAAV5-hSyn-eYFP, rAAV5-hSyn-Jaws-KGC-GFP-ER2 or rAAV5-hSyn-hChR2(H134R)-eYFP in Superior Colliculus (SC) and implanted with optic fiber in the VTA performed the real time place preference (rtPP). The rtPP experiment was conducted in an apparatus (spatial place preference; BioSEB) consisting of two adjacent chambers (20 × 20 × 25 cm) with dot (black) or stripe (gray) wall patterns, connected by a lateral corridor (7 × 20 × 25 cm) with transparent walls and floor. The dot chamber was always associated to rough floor, while the stripe chamber with smooth floor. The illumination level was uniform between the two chambers and set at 10 – 13 lux. Imetronic (Pessac, France) tracking software was used to track animal's movements, the time spent within each chamber and to deliver optogenetic protocols. The eYFP-control, Jaws and ChR2-expressing mice were placed in the apparatus and were free to explore both chambers during 10 min. One chamber was systematically associated with a high bursting optogenetic stimulation protocol for ChR2-expressing mice (burst of 5 pulses of 4 ms at 20 Hz every 250 msec), or constant light-ON inhibition for Jaws-expressing mice, while the other was not associated with any optical stimulation protocol. The chamber associated with the light stimulation or inhibition was counterbalanced to avoid any internal bias due to the cues of the compartment.

After the task, the animals were sacrificed and the viral infection was verified. If no infection was noticed or the optic fiber not in the right area, the mice were excluded from the batch. The apparatus was cleaned using 70% ethanol after each session.

Long-term social habituation/novelty exploration

An experimental cage similar to the animal's homecage was used for this task. The bedding was replaced after each trial. During the habituation phase (4 days, day 1 – 4), all eYFP-control and ChR2-expressing mice were plugged to the optic fiber cable but did not receive optogenetic stimulation protocol. The experimental mice were placed in the cage with an unfamiliar conspecific (unfamiliar juvenile mouse, C57Bl/6J, 3 – 4 weeks old, s1). The animals were let free to explore the cage and to interact with each other for 15 min. At the end of the trial, the experimental and stimulus mice were returned to their homecage. For four consecutive days the experimental mouse was exposed to the same conspecific (s1) and

habituated to the environment and the social stimulus. Day 5 consisted in the novelty phase. The eYFP and ChR2-expressing mice received optical stimulation (burst of 8 pulses of 4 msec light at 30 Hz every 5 sec; Imetronic, Pessac, France) during all the duration of the free interaction. An unfamiliar conspecific (s2) was placed with the experimental mouse in the cage for 15 min to allow direct interaction. In total, the experimental mice were exposed to two different conspecifics: one social stimulus repeatedly presented from day 1 – 4 (habituation phase, s1) and a second mouse at day 5 (novelty phase, s2). During the social habituation/novelty exploration task, nonaggressive interaction was scored (experimenter blind to the viral injection) when the experimental mouse initiated the action and when the nose of the animal was oriented towards the social stimulus mouse only. The time interaction was used to calculate the Index Time Social interaction as: $\frac{Interaction\ day\ 5^{Light}}{Interaction\ day\ 5^{Light} + Interaction\ day\ 4^{No_Light}}$.

After the task, the animals were sacrificed and the viral infection was verified. The optic fiber integrity was checked again by controlling the light power. If no infection was noticed or the optic fiber not in the right area, the mice were excluded from the batch. The apparatus was cleaned using 70% ethanol after each session.

Ex vivo slice physiology

200 – 250 µM thick horizontal midbrain slices were prepared from adolescence/early adulthood C57Bl/6J WT or DAT-Cre mice: ChR2-expressing WT mice infected in the SC and DAT-Cre mice infected with ChR2 in the SC + AAVrg-pCAG-FLEX-TdTomato in the Nucleus Accumbens (NAc), the dorsolateral Striatum (DLS) or the tail of the Striatum (TS) mice. Subjects were anesthetized with isoflurane/O2 and decapitated. Brains were sliced by using a cutting solution containing: 90.89 mM choline chloride, 24.98 mM glucose, 25 mM $NaHCO_3$, 6.98 mM $MgCl_2$, 11.85 mM ascorbic acid, 3.09 mM sodium pyruvate, 2.49 mM KCl, 1.25 mM NaH_2PO_4, and 0.50 mM $CaCl_2$. Brain slices were incubated in cutting solution for 20 – 30 min at 35°. Subsequently, slices were transferred in artificial cerebrospinal fluid (aCSF) containing: 119 mM NaCl, 2.5 mM KCl, 1.3 mM $MgCl_2$, 2.5 mM $CaCl_2$, 1.0 mM NaH_2PO_4, 26.2 mM $NaHCO_3$, and 11 mM glucose, bubbled with 95% O_2 and 5% CO_2) at room temperature. Whole-cell voltage clamp or current clamp electrophysiological recordings were conducted at 32° – 34° in aCSF (2 – 3 $ml.min^{-1}$, submerged slices). Patch pipettes were filled with a Cs^+-based low Cl^- internal solution containing 135 mM $CsMeSO_3$,

10 mM HEPES, 1 mM EGTA, 3.3 mM QX-314, 4 mM Mg-ATP, 0.3 mM Na_2-GTP, 8 mM Na_2-Phosphocreatine (pH 7.3 adjusted with CsOH; 295 mOsm).

For ChR2-expressing WT mice, putative DA neurons of the VTA were identified accordingly to their position (medially to the medial terminal nucleus of the accessory optic tract), morphology, cell capacitance (> 28 pF) and low input resistance at positive potentials. For DAT-Cre mice DA neurons of the VTA were identified as TdTomato$^+$ cells. Brief pulses of blue light (10 msec) were delivered at the recording site at 10 sec intervals under control of the acquisition software. Cells were helded at -60mV in order to evoke excitatory post-synaptic currents (EPSCs) or at 0 mV to evoke inhibitory post-synaptic currents (IPSCs).

Calcium imaging analysis

Image acquisition and image processing. Imaging was performed using a snap-in fluorescence microscope body (OSFM model L, Doric lenses Inc., Canada). The CE:YAG fiber light source (465 nm LED output, Doric Lenses Inc.) was tuned to less than 2 mW. The field of view corresponding to 350 µm x 350 µm was imaged at a spatial resolution of 650 pixels x 650 pixels and at a frame rate of 6.67 Hz. ImageJ (US National Institutes of Health), Doric Neuroscience Studio (Doric Lenses Inc.) and customized MatLab (MathWorks, Inc.) routines were used for image pre-processing. Images from different behavioral sessions of a given day were concatenated by Stack Sorter on ImageJ. Image frames were corrected for infocal (XY) plane brain motion using Doric neuroscience studio alignment system, and smoothed by Kalman stack filter on ImageJ. The corrected stacks were inspected for out-of-focal plane (Z) with the following algorithm: correlation coefficients of fluorescent intensities from all pixels were calculated between a given frame and a reference image (average intensity projection of the most stable stack of the day) by image CorrelationJ on ImageJ. If a correlation coefficient of a frame was smaller than 0.9 then the frame was replaced to the average of prior and posterior images. To identify neurons and to detect Ca^{2+} transients, we used a previously published cell-sorting algorithm (Mukamel et al., 2009; Ziv et al., 2013) running on MatLab. Ca^{2+} transients were identified by searching each trace for local maximum that had peak amplitude higher than two standards deviations from the baseline trace. Relative changes in fluorescence of registered images were computed by $F(t)/ F_0 = (F(t) - F_0)/F_0$, where F_0 is the mean image of the entire stack. For the cell alignment between different days, the maximum intensity projection of all stacks of each day was used as a reference. Candidates cells across days that might represent the same neuron were both

manually identified, cell by cell.

Behavioral test. The experimental mice performed both of the free social interaction task and the object exploration task (see direct interaction for *in-vivo* calcium imaging part for details). All behaviors were monitored using a digital camera (Stoelting). The frame rate was 28 frames / sec. The behavior images were synchronized with the Ca^{2+} imaging by an external TTL signal from ANYMAZE interface (Stoelting). Mouse behavioral activity was analyzed manually frame-by-frame and scored including nose-to-nose sniffing, anogenital sniffing and close following for the free social interaction. Only object interaction was scored for the object exploration task.

Data analysis. The neurons were matched between the first day (free social interaction sessions) and the second day (object exploration sessions). The firing rate of each neuron was defined by the sum of the amplitudes of each Ca^{2+} transient per session, divided by the duration of each session. The number of active neurons was computed as following: number of neurons which was active at least one time during one of the sessions, divided by the total number of detected neurons.

Immunohistochemistry and cell counting

ChR2 and eYFP in the SC, CTB 488/CTB 555 in the NAc and the DLS respectively and CAV-Cre in the VTA with AAV-hSyn-DIO-mCherry in the SC ($VTA^{CAV\text{-}Cre}$::$SC^{AAV\text{-}DIO\text{-}mCherry}$) infected mice were anesthetized with pentobarbital (Streuli Pharma) and sacrificed by intra-cardial perfusion of 0.9% saline followed by 4% paraformaldehyde (PFA; Biochemica). Brains were post-fixed overnight in 4% PFA at 4°C. 24 hours later, they were washed with PBS and then 50 µm thick sliced with a vibratome (Leica VT1200S).

Previously prepared slices were washed three times with phosphate buffered saline (PBS) 0.1M. Brain slices were pre-incubated with PBS-BSA-TX buffer (10% BSA, 0.3% Triton X-100, 0.1% NaN_3) for 60 min at room temperature in the dark. Subsequently, cells were incubated with primary antibodies diluted in PBS-BSA-TX (3% BSA, 0.3% Triton X-100, 0.1% NaN_3) overnight at 4°C in the dark. The following day cells were washed three times with PBS 0.1M and incubated for 60 min at room temperature in the dark with the secondary antibodies diluted in PBS-Tween buffer (0.25% Tween-20). Finally, slices were mounted using Fluoroshield mounting medium with DAPI (abcam). In this study, the following primary antibodies were used: mouse monoclonal anti-CaMKII alpha (1/100 dilution, ThermoFisher, MA1-048), rabbit polyclonal anti-mCherry (1/200 dilution, abcam, ab167453) and rabbit polyclonal anti-Tyrosine Hydroxylase (1/500 dilution, abcam, ab6211). The

following secondary antibodies were used at 1/500 dilution: donkey anti-mouse 488 (Alexa Fluor), donkey anti-rabbit 555 (Alexa Fluor) and donkey anti-rabbit 647 (Alexa Fluor). Immunostained slices were imaged using the confocal laser scanning microscopes Zeiss LSM700 and LSM800. Larger scale images were taken with the widefield Axioscan.Z1 scanner.

Cell counting of $mCherry^+$ cells was performed on 50µm thick SC slices from 3 $VTA^{CAV-Cre}$::$SC^{AAV-DIO-mCherry}$ mice (5 slices for each animal). For each slice, images from the SC and PAG were acquired bilaterally along the whole SC dorso-ventral axis. The $mCherry^+$ cells were counted automatically using MetaMorph Software (Molecular Devices) from different field of view. The total percentage of cells located in the different layers of the SC or the PAG was calculated by averaging the total number $mCherry^+$ of each mouse. After CaMKIIa immunostaining onto SC slices, the number of $mCherry^+$/ $CaMKIIa^+$ and $mCherry^+$/ $CaMKIIa^-$ cells were counted.

Drugs and viruses

rAAV5-hSyn hChR2(H134R)-eYFP (Titer ≥ 7×10^{12} vg.mL-1, Addgene), rAAV5-hSyn-Jaws-KGC-GFP-ER2 (Titer ≥ 3.8×10^{12} vg.mL-1, UNC Vector Core), rAAV5-hSyn-eYFP (Titer ≥ 7×10^{12} $vg.mL^{-1}$, Addgene), rAAV5-Ef1α-DIO-hChR2(H134R)-eYFP (Titer ≥ 4.2×10^{12} $vg.mL^{-1}$, UNC Vector Core), rAAV5-Ef1α-DIO-eYFP (Titer ≥ 4.2×10^{12} $vg.mL^{-1}$, UNC Vector Core), rAAV5-hSyn-DIO-mCherry (Titer ≥ 7×10^{12} $vg.mL^{-1}$, Addgene), AAVrg-pCAG-FLEX-tdTomato-WPRE (Titer ≥ 1×10^{13} $vg.mL^{-1}$, Addgene), CAV-2 Cre (Titer ≥ 2.5×10^{11} pp, Plateforme de Vectorologie de Montpellier, PVM), AAV1/2-hSyn-FLEX-GCamp6f-WPRE-SV40 (Titer ≥ 3.8×10^{12} vg.mL-1, UNC Vector Core), AAVrg-Ef1α-mCherry-IRES-Cre (Titer ≥ 7×10^{12} vg.mL-1, Addgene). Cholera Toxin Subunit B (Recombinant), Alexa Fluor™ 488 Conjugate (ThermoFisher Scientific, C22841)**,** Cholera Toxin Subunit B (Recombinant), Alexa Fluor™ 555 Conjugate (ThermoFisher Scientific, C34776).

Statistical analysis

No statistical methods were used to predetermine the number of animals and cells, but suitable sample sizes were estimated based on previous experience and are similar to those generally employed in the field. The animals were randomly assigned to each group at the moment of viral infections or behavioral tests. Statistical analysis was conducted with

MatLab (The Mathwork) and GraphPad Prism 7 (San Diego, CA, USA). Statistical outliers were identified by using the criterion $Mean_{Value} \pm 3 \times Std_{Value}$ and excluded from the analysis. The normality of sample distributions was assessed with the Shapiro–Wilk criterion and when violated nonparametrical tests were used. When normally distributed, the data were analyzed with independent t test, paired t test, while for multiple comparisons one-way ANOVA and repeated measures (RM) ANOVA were used. When normality was violated, the data were analyzed with Mann–Whitney test. For the analysis of variance with two factors (two-way ANOVA, RM two-way ANOVA and RM two-way ANOVA by both factors), normality of sample distribution was assumed, and followed by Bonferroni-Holm correction test or Bonferroni post-hoc test. All the statistical tests adopted were two-sided. When comparing two samples distributions similarity of variances was assumed, therefore no corrections were adopted. Data are represented as the $Mean \pm s.e.m.$ and the significance was set at $P < 0.05$.

Reference for the methods

Mukamel, E. A., Nimmerjahn, A. & Schnitzer, M. J. Automated analysis of cellular signals from large-scale calcium imaging data. *Neuron* **63**, 747-760, doi:10.1016/j.neuron.2009.08.009 (2009).

Ziv, Y. *et al.* Long-term dynamics of CA1 hippocampal place codes. *Nature neuroscience* **16**, 264-266, doi:10.1038/nn.3329 (2013).

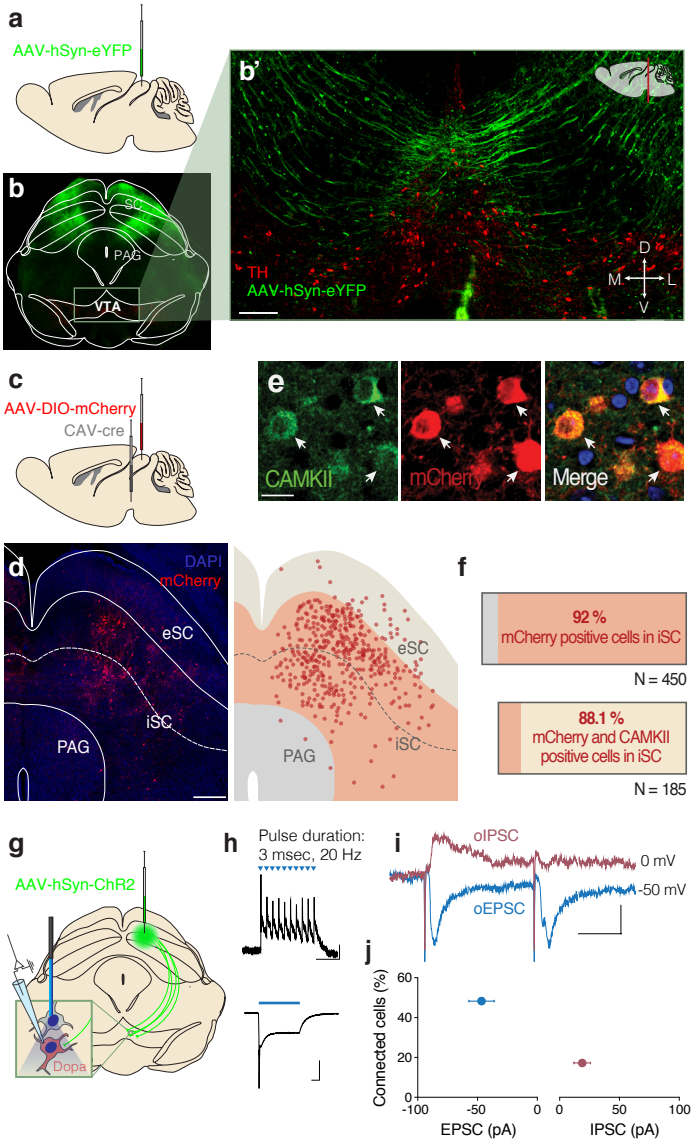

Figure 1. Prévost-Solié, Contestabile et al. 2019

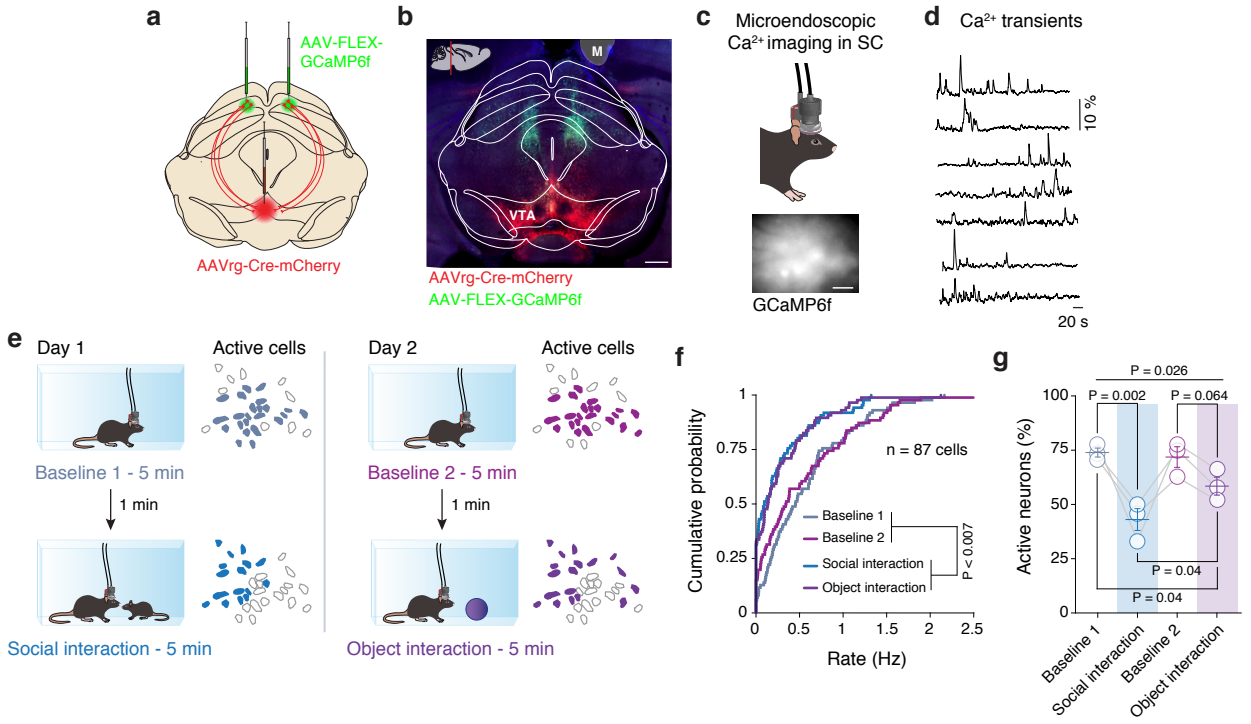

Figure 2. Prévost-Solié, Contestabile et al. 2019

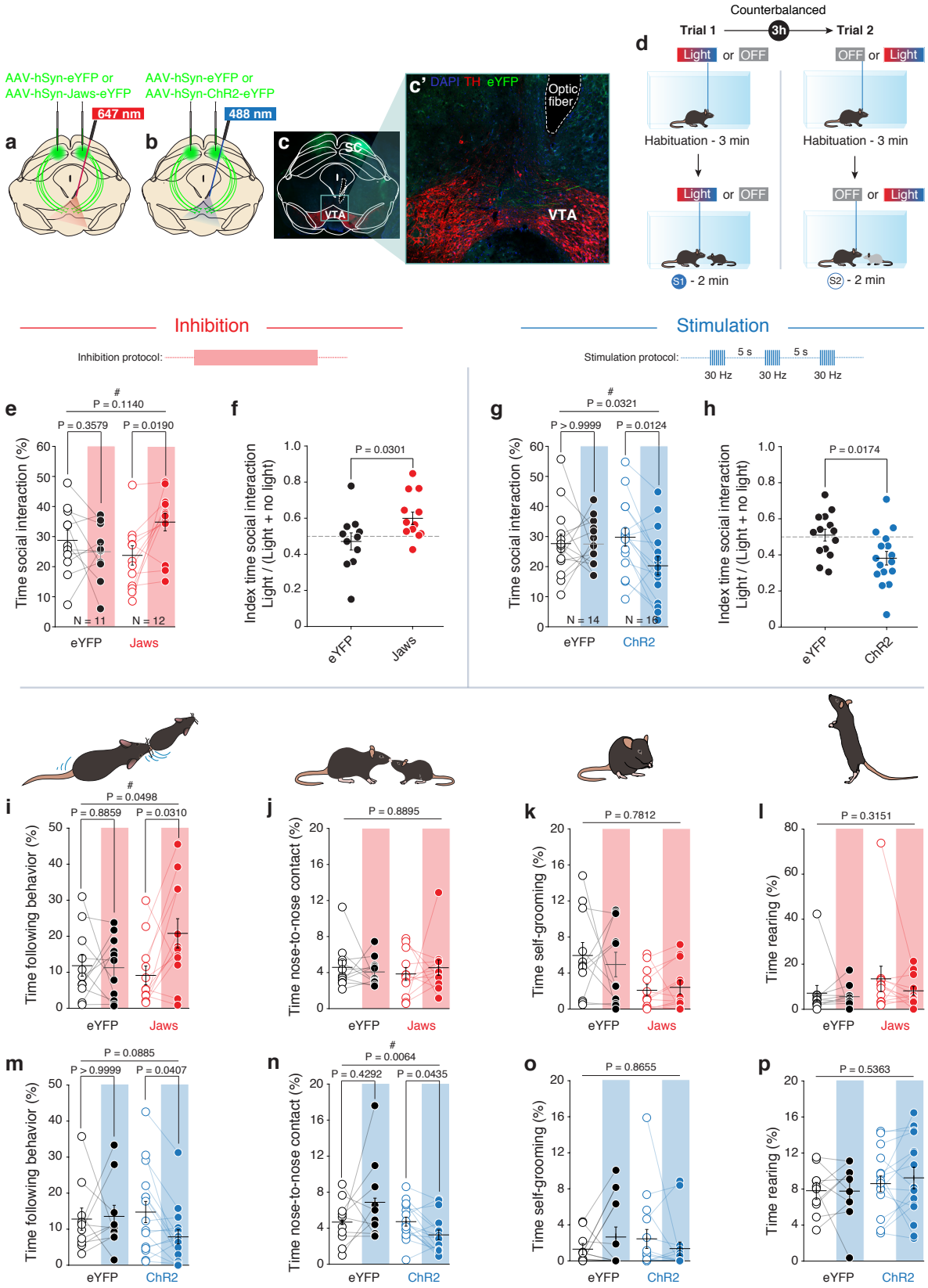

Figure 3. Prévost-Solié, Contestabile et al. 2019

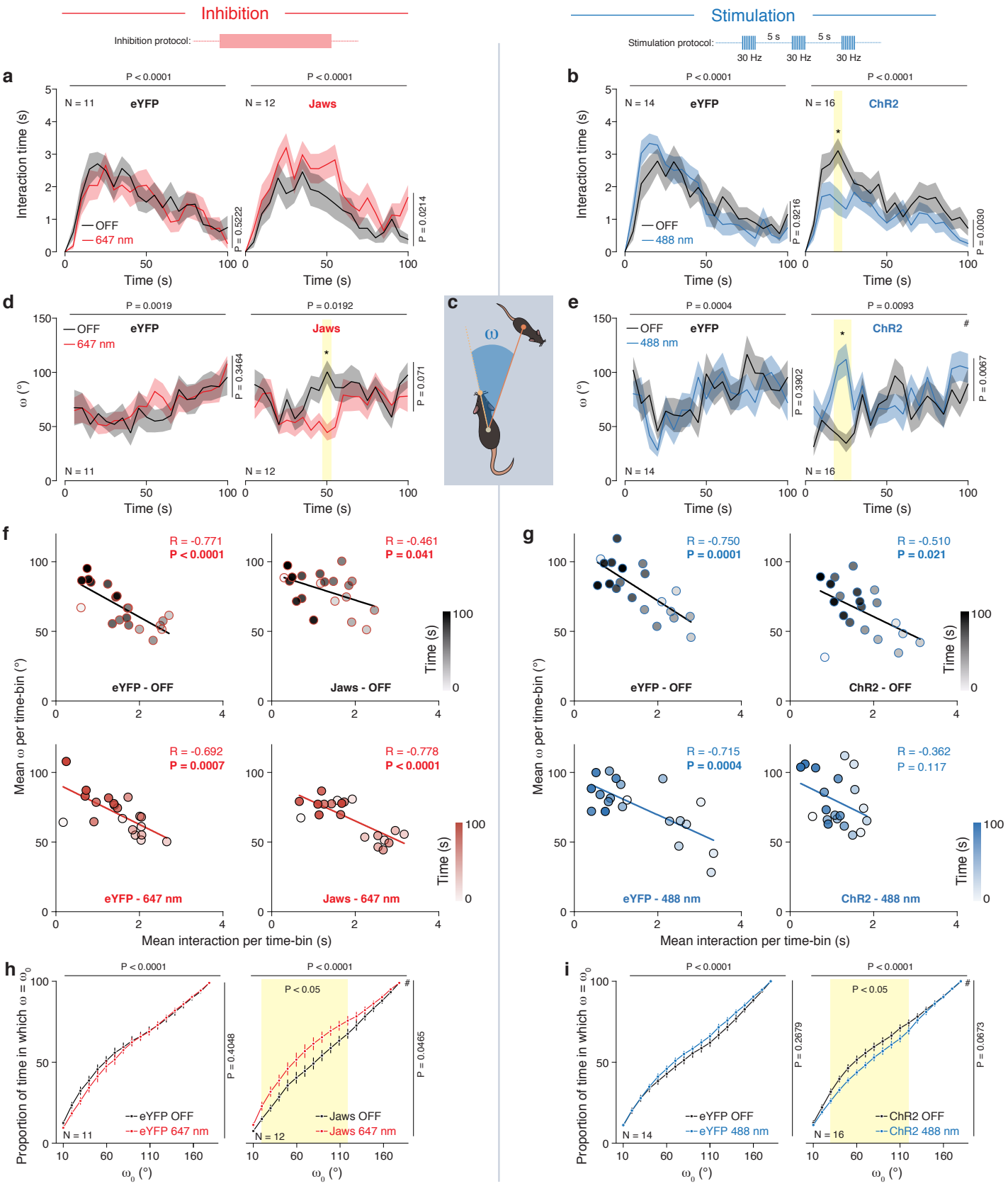

Figure 4. Prévost-Solié, Contestabile et al. 2019

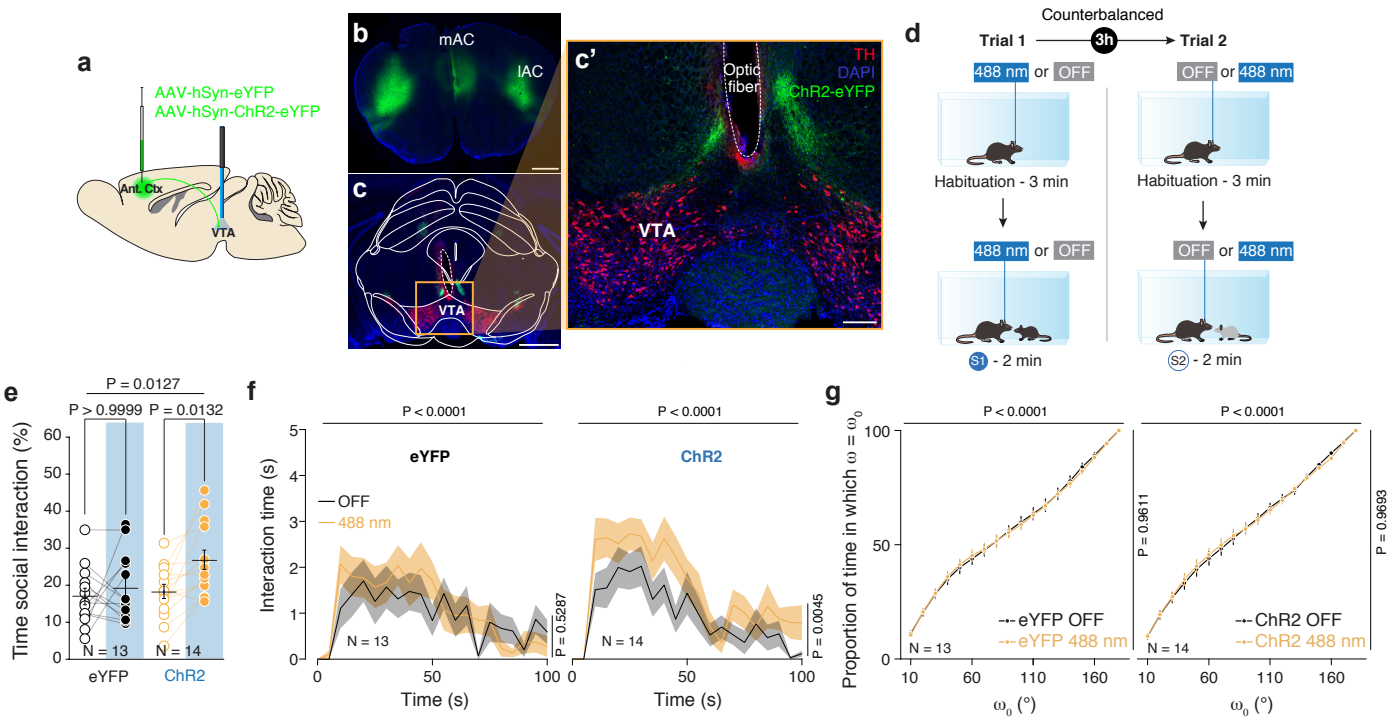

Figure 5. Prévost-Solié, Contestabile et al. 2019

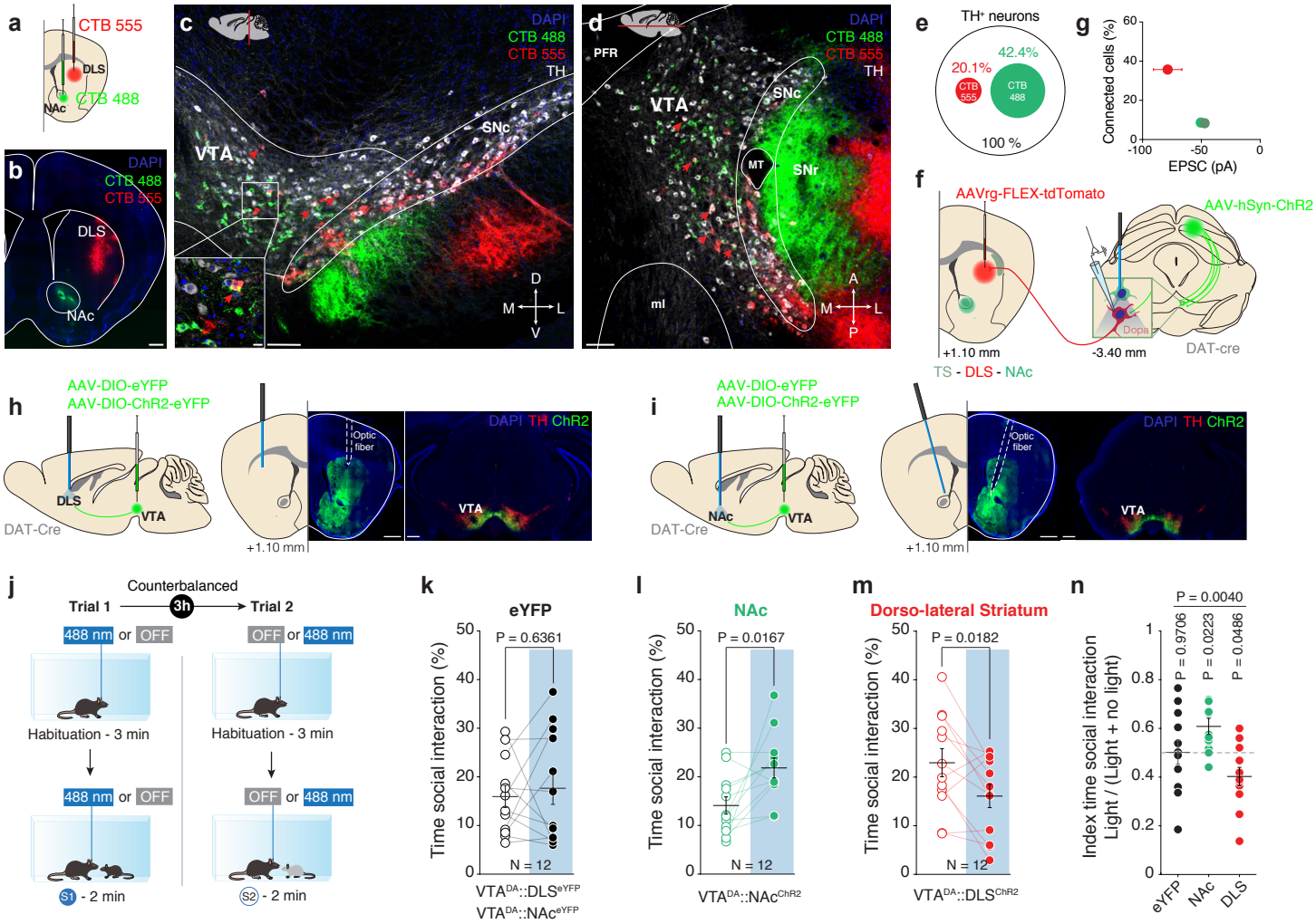

Figure 6. Prévost-Solié, Contestabile et al. 2019